IDENTIFICATION OF EWS-FLI1 REGIONS NECESSARY FOR EWING SARCOMA PROLIFERATION

APPROVED BY SUPERVISORY COMMITTEE

David McFadden, M.D., Ph.D.

James Amatruda, M.D., Ph.D.

Steve McKnight, Ph.D.

Hongtao Yu, Ph.D.

IDENTIFICATION OF REGIONS OF EWS-FLI1 NECESSARY FOR EWING SARCOMA PROLIFERATION

by

ALBERTO BREMAUNTZ ENRIQUEZ

DISSERTATION

Presented to the Faculty of the Graduate School of Biomedical Sciences

The University of Texas Southwestern Medical Center at Dallas

In Partial Fulfillment of the Requirements

For the Degree of

DOCTOR OF PHILOSOPHY

The University of Texas Southwestern Medical Center at Dallas

Dallas, Texas

December, 2021

IDENTIFICATION OF REGIONS OF EWS-FLI1 ESSENTIAL FOR EWING SARCOMA PROLIFERATION

Publication No. _____

Alberto Bremauntz Enriquez, Ph.D.

The University of Texas Southwestern Medical Center at Dallas, 2021

Supervising Professor: David McFadden, M.D., Ph.D.

Ewing sarcoma is pediatric bone malignancy defined by a translocation between EWS and ETS family transcription factor. EWS-FLI1 (EF) is the most common translocation and codes for a novel transcription factor that combines the N-terminus of EWS, which contains LC domain comprised of tyrosine rich peptide repeats, and C-terminal portion of FLI1, which contains the ETS DNA binding domain. EF is a key transcriptional regulator known to both activate and repress genes. While understanding of the molecular mechanism by which EF controls transcription have become clearer, targeted therapeutic interventions against EF or its transcriptional program have yet to make clinical impact. This is due in part to a poor understanding of how the N-terminus of EWS is contributing to the oncogenic program and a

disparate range of reported effects after EF depletion on Ewing sarcoma cells. This report shows the adaptation of two inducible degron systems, Small Molecule Assisted Shut-Off (SMASh) and Auxin-inducible degron (AID), into the endogenous locus of EF in a series of Ewing sarcoma cell lines to define the phenotype of EF depletion. Across multiple cell line and degradation mechanisms, EF depletion in Ewing sarcoma cells leads to decreased cell proliferation through G1/S arrest that can be rescued through re-expression of EF. Having established a baseline for EF depleted cells, I developed a proliferation-based assay to test the functionality of mutant EF constructs on their ability to drive proliferation in the setting of endogenous EF depletion. I tested a series of EF truncations, with single or multiple exon deletions in the EWS portion of the translocation. Expression of EF constructs with loss of any single exon was tolerated and allowed for continued proliferation, but loss of at least exons 1-4 on the N-terminus and loss of exons 5-7 from the C-terminus resulted in non-functional EF constructs. Given that there appear to be redundant elements within the N-terminus of EF, I tested truncated and mutant version of a minimal rescue construct containing only exon 1-5 of the N-terminus of EF. Mutation of only 3 tyrosines to serine within the minimal construct was sufficient to prevent proliferation in Ewing cell lines.

TABLE OF CONTENTS

PRIOR PUBLICATIONS

V.H. Cruz, E.N. Arner, W. Du, **A. Bremauntz**, R.A. Brekken. *Axl-mediated activation of TBK1 drives epithelial plasticity in pancreatic cancer*. JCI Insight. 2019. **5**(9): e126117.

J. Chen, **A. Bremauntz**, L. Kisley, B.Shuang, C.F. Landes. *A Super-Resolution mbPAINT for Optical Localization of Single-Stranded DNA*. ACS Appl Mater Interfaces. 2013. **5**(19): p.9338-43.

LIST OF TABLES & FIGURES

LIST OF DEFINITIONS

AID- Auxin inducible degron

BAF- Barrier to autointegration factor

CAS9- CRISPR associated protein 9

CCND1- Cyclin D1

CRISPR- Clustered regularly interspaced short palindromic repeats

DKK1- Dickkopf WNT Signaling Pathway Inhibitor 1

DKK2- Dickkopf WNT Signaling Pathway Inhibitor 2

EGR2- Early Growth Response 2

ERG- ETS Related Gene

ETS- E26 Transformation Specific

EWS – EWS RNA Binding Protein

F-box- target binding domain in E3 ubiquitin ligase complex

FLI1- Friend leukemia integration factor 1

FET- FUS, EWS, TAF15 protein family

FPKM- Fragments Per Kilobase of transcript per million mapped reads

Gal4- a positive regulator of gene expression of galactose-induced genes

H3k27- Histone H3 amino acid number 27, lysine

HSF1- Heat shock transcription factor 1

IAA- Inole-3-acetic acid

5-Ph-IAA- 5-Phenyl- indole-3-acetic acid

KRAB- Krüppel-associated box transcriptional repression domain

MS2- bacteriophage MS2 coat protein

MSC- Mesenchymal stem cell

NIH 3T3- Mouse embryo fibroblasts

NKX2.2- NK2 Homeobox 2

NR0b1- Nuclear Receptor Subfamily 0 Group B Member 1

NS3- Hepatitis C nonstructural protein 3

NSG- Next Generation Sequencing

P27- Cyclin dependent Kinase Inhibitor 1B

P51- Tumor protein 51

P53- Tumor suppressor protein 53

P65- nuclear factor NF-kappa-B p65 subunit

P300- E1A binding protein P300

pRB- phosphorylated Retinoblastoma protein

PI- propidium iodide

sgRNA- single guide RNA

SMASh- Small molecule assisted shut-off

STAG2- Stromal Antigen 2

TAF15- TATA-box binding protein associated factor 15

TIR1- Transport Inhibitor response 1 protein

V5- Simian virus 5 epitope tag

VP64- 4 copies of Herpes Simplex Viral protein 16

WT- Wild type

ZsGreen- green fluorescent protein

CHAPTER ONE
Introduction

1.1 Ewing sarcoma in the clinic

In 1921, Dr. James Ewing reported a case study of a 14-year-old girl who had presented with a mass in her upper arm that had appeared secondary to an ulnar fracture. She was originally diagnosed with "osteogenic sarcoma" and after being unresponsive to Coley's toxin treatment, radium treatment was able to cause a decrease in tumor size. When the mass returned, a tissue sample revealed the tumor was comprised of "small polyhedral cells with pale cytoplasm [and] small hyperchromatic nuclei". Unfortunately, by this time the disease had metastasized, and the patient passed away. Dr. Ewing classified this case along with similar "round cell sarcoma[s]" found in other children as a distinct malignancy he called "diffuse endothelioma of bone" [1]. Building upon these reports, a subset of osteogenic sarcomas and other histologically similar soft tissue sarcomas comprise what is today known as the Ewing sarcoma family of tumors.

The cases of Ewing sarcoma resemble the original reports described by Dr. Ewing with the peak incidence of this disease in individuals between the ages of 10 and 20. Ewing sarcoma is the second most common pediatric bone malignancy and accounts for 2-3% of total cancer cases in children (2). Despite the relative rarity of this disease, the burden of disease on patients during treatment and even after survival is high. Local surgical resection is a first line treatment, but due to the threat of undetected disseminated disease multiple cycles of

chemotherapy are given to patients with localized disease. Even with improvements in chemotherapy regiments, five-year survival for individuals with localized diseases is still only 70-80%. For patients who have metastatic disease the prognosis is even worse with only 30% survival at five years (3,4). Even the patients who overcome their illness may still suffer from secondary neoplasms or other morbidities as consequence of their treatment (5). There is still a clear need for more targeted and effective therapies that can help increase survival and decrease toxicity for these patients.

1.2 Genetics of Ewing sarcoma

A key breakthrough in the understanding of the oncogenic program of Ewing sarcoma, is the discovery of the t(11;22)(q24;q12) translocation that fuses the RNA associated EWS and ETS family transcription factor FLI1 (6). This was an indication that Ewing sarcoma is driven by a novel chimeric transcription factor formed by the fusion of a transcriptional activating domain on N-terminal portion of EWS and the conserved ETS DNA binding domain on the C-terminus of FLI1 (6). Subsequent tumor sequencing has revealed additional translocations involving other FET and ETS family members such EWS-FEV and FUS-ERG (7,8,9). While there is variability in the translocation events within these tumors, up to 90% of tumors contain the EWS-FLI1 (EF) translocation. Despite a variability in the breakpoint between EWS and ETS transcription factors, all tumors containing EWS retain at least the first 7 exons of EWS in the translocation (6,7).

Multiple comprehensive sequencing studies have attempted to identify additional key mutations in Ewing sarcoma. These studies have utilized whole genome sequencing or RNA sequencing to investigate genetic changes in large sets of tumors. Two mutations, apart from the translocation, were identified throughout this work to have an impact on disease progression: STAG2 and p53. A loss of function mutations in STAG2 were identified in upwards of 15% of sequenced tumors and were associated with more advanced disease. Loss of function mutations p53 in conjunction with STAG2 loss was associated with a worse prognosis (10, 11, 12). Throughout these EF sequencing studies, Ewing tumors had relatively few mutations in comparison to other cancers.

1.3 EWS-FLI1 function is context dependent

Given that the EF translocation appears to be to most common and important genetic event in Ewing sarcoma, an understanding of the role of EF in Ewing biology is essential for the treatment of this disease. Early studies tried to tease out whether EF was recapitulating the function of either FLI1 or EWS, or if the EF had a novel function by replacing the transcriptional activating domain of FLI1 with the N-terminus of EWS. One piece of evidence that EF had a novel function was the finding that only the translocation product EF, and not EWS or FLI1 was capable of inducing colony formation in NIH 3T3 cells (13). Further evidence of the importance of the N-terminal region was established when an EF translocation construct with deletion of the first 264 amino acids of EWS failed to transform NIH 3T3 cells (15). Another study using a transcriptional reporter assay showed the N-

terminus of EWS attached to Gal4 demonstrated increased transcriptional activation as compared to the N-terminal transcriptional activating domain of full length FLI1 (14).

An understanding that EF activity was dependent on the cellular context where the translocation occurred, began to develop when it was reported that EF caused p53-dependent arrest in human fibroblasts (16, 17). This finding spurred groups to try to identify the cell lineage where the translocation induced oncogenesis. Another study aimed to gain insight regarding a potential cell line of origin by transforming multiple primary murine stem cells with EF. Among their candidates, only bone marrow derived mesenchymal stems cells (MSC) expressing EF were able to form tumors with Ewing like features (18). Further studies showed that primary human MSCs transformed with EF were able to produce tumors with histological and transcriptional similarities to Ewing tumors (19, 20). Evidence for MSCs as a cell line of origin were bolstered by a comparison of the microarray gene signature of multiple stem cell populations with those of siRNA knockdown of EF in patient derived Ewing cell lines. This analysis showed that the gene signature of EF depleted A673, EW24, and SK.N.MC clustered with those of MSCs and not other stem cell populations (21).

Phenotype of EF depletion in patient derived Ewing cell lines:

An alternative methodology to studying the function EF has utilized multiple siRNA approaches to deplete EF in patient derived Ewing cell lines. This method ensures a more relevant cellular context than putative cell lines of origin for understanding EF biology. Early studies began to establish a critical role for EF in Ewing cell proliferation. Antisense

oligonucleotides were used to deplete endogenous EF levels in SK.N.MC cells resulting in an accumulation of cells in G1 phase of the cell cycle, decreased cell growth, and inhibited tumor formation (22, 23). However, subsequent EF knockdown studies using different cell lines have shown a series of conflicting phenotypes of depletion. Some groups have reported a senescence-like phenotype that corresponds with p27&p57 activation and pRB activation after siRNA knockdown of EF in SK-ES and RD-ES cells (24). Meanwhile other groups have seen no changes in proliferation, but impaired colony formation after siRNA knockdown of EF in A673 cells (25). Given the potential off-target effects and differing levels of EF knockdown across these studies, there is still a need to better define the phenotype of EF depletion in Ewing cells.

1.4 EWS-FLI1 as a transcriptional regulator

Since EF appears to function as chimeric transcription factor, groups have studied the role of EF in both patient derived stem cells and MSC to identify individual EF targets as well as broader mechanisms of transcriptional regulation. Microarray analysis of A673, TC71, and EWS502 cells after siRNA knockdown of EF identified NKX2.2 as a highly upregulated target and NR0B1 as a highly downregulated target of EF (25,26). Microarray analysis of Ewing cell lines and tumors also identified DKK2 and DKK1 as upregulated and downregulated genes. Expression of EF in MSC showed a repression of DKK1 and increased expression DKK2, despite only DKK2 having a putative ETS-binding site (27). These studies show that EF has a capability of both activating and repressing gene targets.

The ability to track all the binding sites of EF throughout the genome, became an important tool for understanding the mechanism through which EF regulates transcription. Sequencing of chromatin immunoprecipitation of FLI1 in A673 cells demonstrated binding of EF preferentially at GGAA microsatellite repeats at gene promoters. Surprisingly, this preference was stronger than that of canonical ETS binding sites, with sites exceeding 9 GGAA repeats being the most enriched. Binding of EF to these promoter regions was associated with increased transcription of those genes. A characteristic example of one of these regions is the GGAA microsatellite upstream of NR0B1 (28,29).

Further analysis has shown that EF regulates transcription by altering chromatin states at different sites. EF can activate genes downstream of large GGAA microsatellite repeats large through the recruitment of p300 and subsequent histone acetylation (H3K27). On native ETS binding sites (single GGAA), EF can replace ETS transcription factors leading to repression of those genes. (31). Subsequent studies have shown the presence or absence of EF at leads to epigenetic changes at GGAA microsatellites repeats or traditional enhancers to regulate transcription (32,33). Recent studies have implicated the BAF complex as an EF partner that can be recruited for chromatin opening at enhancer sites as a mechanism of activating transcription (43). Finally, targeted transcriptional repression through CRISPRi that localized a nuclease inactivated Cas9 (dCas-9) with an attached KRAB repressor domain to EF binding regions has been shown to be sufficient in its ability to block EF dependent transcripts at GGAA microsatellites (34).

1.5 Role FET LC domains in Ewing sarcoma biology

FUS, EWS, and TAF15 are all part of the FET family of RNA binding proteins. This family of proteins contains an N-terminal low complexity (LC) region which is comprised of S/G Y S/G peptide repeats (35). This family of RNA binding proteins was identified in RNA granules in cells treated with biotinylated-isoxazole. Their LC domains were determined to mediate their recruitment to these granules and potentiate the concentration dependent formation of fibrils and hydrogels (38, 39). Subsequent studies have demonstrated hydrogels made from the LC domain of FET proteins can bind the unphosphorylated C-terminal domain of RNA polymerase II (40).

The LC domain of FUS has been the most well characterized of the FET proteins, with recent reports of outlining the structure of the FUS LC fibril core as a 57 aa stretching from aa 39-95 (41). FUS bound to Gal4 has been shown to be a transcriptional activator in luciferase reporter assays and FUS-FLI1 can potentiated to form fibrils in the presence of the NR0B1 GGAA microsatellites at lower concentrations than without DNA (40).

Meanwhile, the N-terminal domain of EWS has been known to allow for homotypic and heterotypic interactions both in vivo and in cells between full length EWS and EWS-FLI1 (37). Transcriptional reporter assays have also shown that EWS-ATF1 is dependent primarily on the N-terminal tyrosines within the LC domain for transcriptional activation (43). Together these findings point to unique biology of the LC domains in vitro.

More recently there have been studies implicating LC dependent phase separation in the transcriptional regulation of EF in cells. A study exploring the role of DNA bound LC domains showed halo tagged EF forms LC hubs at GGAA microsatellites in A673 cells. These hubs have shown to be dependent on DNA binding and the presence of tyrosines in N-terminus of EWS (42). Studies of EF mediated chromatin remodeling show an increasing loss of the Ewing transcriptional fingerprint after transduction of MSC with a series of EF constructs with increasing tyrosine to serine mutation in LC region. This study has also reported on two SYGQ rich regions, in exons 4 and 7 of EWS that can each be expressed as the sole EWS component in frame with the FLI1 in MSC to reproduce a Ewing-like transcriptional profile (44). Finally, transcriptome analysis of A673 expressing a series of N-terminal EWS truncations & mutants has attempted to link subsets of EF driven transcripts to regions of the EWS (45).

1.6 Conclusion

Since its identification, EF has been shown to have unique properties than cannot be attributed to the normal function of either full length EWS or FLI1. EF appears to function as a distinct transcription factor with studies showing increased transcriptional activation (14,15) and unique transcriptional targets (29-33). While there have been multiple reports on “essential” transcriptional targets of EF (25-27), clinically relevant therapeutic interventions are still lacking. The discrepancies in reported EF depletion phenotypes across cell lines and publications further complicates understanding of EF transcriptional regulation by failing to provide a reconcilable picture of EF function across various systems (22-25). As a result,

there is a need to establish more robust and reproducible methods of EF depletion for identification of essential targets.

Across multiple studies, there is evidence that the N-terminal portion containing the LC domain of EWS is essential for EF function. The tyrosine residues within this region appear to be necessary for both transcriptional activation and condensate formation on microsatellite repeats (42, 43). While this data implicates LC mediated phase separation in the transcriptional regulation of Ewing sarcoma, there is still little evidence linking long term Ewing sarcoma proliferation to the interactions mediated by this domain.

CHAPTER TWO
Defining the phenotype of EWS-FLI1 depletion in Ewing sarcoma cells

2.1 Engineering inducible degradation of EWS-FLI1

To establish a phenotype for EWS-FLI1 depletion, inducible degron tags were introduced into the endogenous EF locus of Ewing sarcoma cell lines. Using CRISPR-Cas9 induced homologous recombination the SMASh system was targeted to the 3' end of FLI1 in A673 cells (Fig 2.1A). The SMASh system (44) is a self-cleaving tag comprised of a Hepatitis C viral (HCV) NS3 protease, NS3 cleavage recognition sequence, and a degron domain. Upon HCV inhibition with a small molecule, the tag cleavage is inhibited and the attached degron leads to degradation of the tagged protein (Fig 2.1B). Single cell clones were picked and sequenced to verify targeting of the FLI1 allele. To ensure that all EF proteins could be degraded, only clones that had all copies of the EF allele properly targeted were carried forward into future experiments

I treated sequence validated A673 SMASh clones with Danoprevir, an HCV protease inhibitor, to test endogenous EF depletion. Increasing doses of Danoprevir resulted in depletion of the endogenous EF band and a shift in detectable FLI1 levels from the to a high molecular weight species (Fig 2.2A). This high molecular weight species matched the size of the EF with the attached SMASh degron tag. To rule out any dominant negative effects of the EF-SMASh species, I transduced wildtype A673 cells with a lentivirus containing an inducible pZIP system for expression of the EF-SMASh construct with an uncleavable linker and removed the degron domain. The pZIP system allows for tetracycline dependent

expression of a stable EF construct that would mimic the high molecular weight EF^{SMASh} band. After selection of A673 pZIP EF^{SMASh} cells, I induced EF^{SMASh} expression with two doses of Doxycycline over a 48h period (Fig 2.3 C). Seeing that the inducible construct did show similar expression levels of EF^{SMASh} to those seen after Danoprevir mediated EF depletion, I tested to see if co-expression of endogenous EF and EF^{SMASh} resulted in any proliferation defects. I grew A673 pZIP EF^{SMASh} cells in doses of Doxycycline or vehicle over a 5-day period and then compared proliferation through cell titer glow. Co-expression of EF^{SMASh} and endogenous EF resulted in cells having no defects in proliferation as compared to cells only expressing endogenous EF (Fig 2.3D).

To ensure that the phenotype observed using EF depletion with the SMASh systems was not confounded by the higher molecular weight EF species, the AID system (45) was adpated as an alternative inducible degron tag. Using the same targeting strategy as for SMASH, sequence verified single cell clones of A673 AID cells were obtained (Fig 2.1A). To introduce the necessary plant F-box protein required by the AID system, A673 AID clones were transduced with a lentiviral construct expressing V5-tagged TIR1 and co-expressing ZsGreen. Transduced A673 AID clones were subsequently sorted for high expression using ZsGreen as fluorescent marker. I next treated A673 AID+TIR1 cells with increasing doses of IAA to induce EF depletion. After 24h of IAA treatment, I looked at EF levels using FLI1 immunoblotting and saw a dose dependent depletion of EF with no other observable FLI1 species (Fig 2.2B).

I next sought to compare the dynamics of depletion between the two systems. I treated a series of A673 SMASh clones with 1µM Danoprevir over a 72h period taking samples at multiple time points to determine the level of endogenous SMASh depletion over time. Depletion of endogenous EF and accumulation of EF^{SMASh} species was detectable as early as 2h after start of treatment. Depletion of half of the endogenous level of EF was visible at 12h and full depletion was visible after 24h (Fig 2.2C). A673 AID clones were treated with 100µM IAA over a 48h period, with samples taken at multiple time point between 1h and 48h. In contrast to the SMASh system, the AID systems showed endogenous depletion as early as 1h after treatment with IAA and was maintained throughout the treatment time course (Fig 2.2D). This data indicates the AID system is a faster acting degradation system than SMASh. I next tested to see if protein depletion was reversible in both systems, by checking if EF levels would return after a washout of compound. I treated A673 SMASH and AID clones with corresponding compound for 72h, then washed plates and maintained cells on drug-free media for at least 24h. Western blots of lysates from A673 SMASh and AID 24h after washout showed re-expression of endogenous EF (Fig 2.2 C,D). Lysates from A673 SMASh showed no expression of the higher molecular weight EF^{SMASh} band after 24h of washout and had incremental increases in re-expression of EF between 24h and 48h after drug washout (Fig 2.2 C, D).

To ensure that EF depletion phenotype was not due to cell specific effect, the endogenous EF locus of additional Ewing sarcoma cell lines was targeted with degron tags. A673, TC32, and SK.N.MC cells were targeted as described above with a series of AID and SMASh targeting

vectors. Multiple A673 SMASh clones with a variety of epitope tags were successfully targeted, however targeting of TC32 and SK.N.MC cells with a SMASh containing an epitope tag resulted in the isolation of clones that all had duplication of the EF allele. Only after alteration of the targeting strategy to include no additional epitope tags in the SMASH targeting constructs, were properly targeted SMASh clones of TC32 and SK.N.MC cells with no EF allele duplication successfully isolated (Table 1). I validated EF depletion in all newly generated SMASh cells by treatment with Danoprevir for 24h and immunoblotting for FLI1. As I had seen with all previously targeted A673 SMASh lines, induced EF depletion in TC32 and SK.N.MC SMASh cells resulted in the previously observed shift from the endogenous EF to a higher molecular weight EF^{SMASh} species (Fig 2.2D, E).

2.2 EF depletion leads to decreased proliferation through G1/S arrest

EF depletion with either the AID or SMASh system resulted in noticeable changes in cell morphology and growth rate. Across all targeted Ewing cell lines, there was a notable flattening and elongation of cells following EF depletion. This phenotype was particularly striking in TC32 and SK.N.MC SMASh cells, where cells took on an almost translucent appearance and greatly increased in size (Fig 2.3A). Since there had been multiple reported effects of EF depletion on proliferation, I decided to pass a series of AID or SMASh clones on either vehicle or compound over a 6-day period. A673 WT cells that have no degron system had no noticeable change in proliferation when treated with Danoprevir or IAA (Fig 2.3B). A673 SMASh and AID cells had a decrease in proliferation after EF depletion with no noticeable cell death present in the EF depleted cells. SK.N.MC an TC32 SMASh cells

showed even more potent proliferation defects after EF depletion, again with no noticeable cell death (Fig 2.3B). While there was some variation in the intensity of both the morphological and proliferation effects, especially between A673 and other Ewing cell lines, all Ewing cells had decreased proliferation following EF depletion.

To determine the cause of decreased proliferation, I analyzed cells' progress through the cell cycle using flow cytometry. I treated A673 AID and A673 SMASh cells with either IAA or vehicle, and A673 SMASh cells with either Danoprevir or vehicle for 24h. After treatment, I fixed the cells in ethanol and stained cells with propidium iodide (PI). Using a flow cytometer, I analyzed the distribution of cells throughout the cell cycle. Vehicle treated A673 AID and A673 SMASh had a distribution of ~60% of counted cell in G1, ~5% of cell in S, and ~35% of cells in G2/M. Upon induced EF depletion with either degron system, the percentage of cells accumulated in the G0/G1 phase increased to nearly 80% and corresponding S and G2/M levels decreased (Fig 2.4A, B).

Given that TC32 and SK.N.MC cells had a more profound phenotype, I repeated the cell cycle analysis in these cell lines with Danoprevir or vehicle treatment. As with the A673 AID or SMASh cells, there was an accumulation of cells at G0/G1 phase after depletion (Fig 2.3C-E). The percentage of cells in G0/G1 correlated with the intensity of the flattening phenotype, with TC32 and SK.N.MC cells having a higher total percentage of cells in the G0/G1 phase after depletion (Fig 2.3C-E). Since different Ewing cell lines and different degron systems all converged on same proliferation and G1/S cell cycle arrest phenotype, it

is likely a direct result of endogenous EF depletion and not an artifact of the method of depletion.

Using Mutated TIR1 to increase AID system sensitivity to 5-Ph-IAA treatment:

Recently, reports of TIR1 mutation in the binding pocket of IAA have been described that increase sensitivity to IAA analogue such as 5-Ph-IAA (50). I transduced A673 AID clones with two TIR1 mutants with reported increased sensitivity to 5-Ph-IAA: TIR1(F74A) & TIR1(F74G) (50). As previously described, the transduced cells were selected for high expression through ZsGreen sorting. I then treated A673 AID+TIR1^{F74AorG} cells with increasing doses of 5-Ph-IAA for 24h. I saw EF depletion at 33nM and 100pM concentrations of 5-Ph-IAA for F74G and F74A respectively. These TIR1 mutants resulted in a substantially improved sensitivity to 5-Ph-IAA. I next checked the cell cycle status of EF depleted cells. I treated A673 AID+TIR1^{F74AorG} cells with either 5-Ph-IAA or vehicle for 24h. I then analyzed PI-stained cells by flow cytometry. As with A673 AID cells expressing wildtype TIR1, EF depletion resulted in an accumulation of cells in G1 phase (Fig 2.5B).

2.3 EF depletion leads to activated and decreased transcripts

Having established two distinct methods of depleting EF in Ewing cells resulting in similar cell cycle and proliferation phenotypes, I sought to characterize the transcriptional changes associated with degron mediated EF depletion. I treated wildtype A673 and two A673 SMASh clones with either vehicle or Danoprevir over a 24h period. I isolated RNA from duplicate samples of A673 cells after 6h, 12h, and 24h of compound or vehicle treatment.

With the help of the Next Generation Sequencing Core at UTSW, RNA samples were validated for quality, prepared into libraries, sequenced, and mapped. I then analyzed the resulting data and defined significant gene changes as those where FPKM changes between the vehicle and Danoprevir condition that either increased or decreased by at least 2-fold. Analysis of total gene changes in EF depleted SMASh clones across each time point showed a time dependent increase in the total number of gene changes in both clones (Table 2 and Fig 2.4A).

To ensure that the transcriptional readout was representative of EF depletion, I followed the expression levels of known EF targets: DKK1 and NR0B1. These genes have been previously documented to be sensitive to EF levels and their expression is respectively repressed and activated by the presence of EF (5,6). Looking at the FPKM changes across A673 SMASh clones between vehicle and Danoprevir treated samples revealed a decrease in transcript levels of NR0B1 following EF depletion. These changes were increased over subsequent time points (Fig 2.6 B). Transcript levels of DKK1 showed a time dependent increase following EF depletion in both A673 SMASH clones (Fig 2.6 C). WT A673 cells that contained no degron system showed no significant transcriptional in either of these genes. Additional known EF genes such as CCND1, CDKN1C, and NKX2.2 were also only significantly altered, per the above criteria, in setting of EF depletion in A673 SMASh clones and were not changed in Danoprevir treated A673 WT cells (Table 3).

To define a core set of transcripts that are dependent on EF expression, I looked at genetic changes in multiple Ewing cell lines. I isolated RNA from two independent SMASh clones of SK.N.MC, TC32, and A673 cells treated with either vehicle or Danoprevir for 24h. Through a commercial sequencing company, BGI, RNA samples were validated for quality, prepared as libraries, sequenced, and mapped. To validate EF dependent transcriptional changes, I looked at the gene changes in DKK1 and NR0B1 across all cell lines. In all A673, SK.N.MC, and TC32 SMASh clones, EF depletion resulted in decreased NR0B1 transcription and increased DKK1 transcription. Having identified known transcriptional changes in EF associated genes, I sought to uncover shared transcriptional changes across all cell lines. Through the same criteria mentioned above, I analyzed the resulting data and identified significant gene changes in both clones for each cell line between the EF depleted and vehicle treated samples for each cell line. As summarized in Fig 2.4D, a total of 264 genes were upregulated throughout all cell line with EF depletion and a total of 192 genes were upregulated under the same conditions.

2.4 In vivo EWS-FLI1 depletion leads to tumor regression

To determine if the G1/S arrest phenotype associated with EF depletion in cells would have the same effect in a tumor, I turned to xenograft models of Ewing sarcoma in nude and NSG mice. I adapted a previously reported method of forming xenografts by mixing cells in a 1:1 mix with Matrigel immediately prior to implantation on nude mice (48). Subcutaneous implantation of A673 SMASh or AID clonal cell lines resulted in viable tumors that maintained EF expression and the histological features of Ewing tumors. After establishment

of palpable tumors in a group of 4 mice, I treated mice twice a day with intraperitoneal (IP) injections of either 30 miligram per kilogram (mpk) Danoprevir or vehicle for 48h. 3h after the final dose, I harvested the tumors, livers, and plasma from all treated mice. Western blot analysis of tumor lysates showed no noticeable EF depletion in the treated samples (Fig 2.7A). With the help of Dr. Noelle Williams and the UTSW Animal Pharmacology Core, analysis of plasma, tumor, and livers samples obtained from treated mice revealed strong accumulation of Danoprevir in the liver and insufficient levels in the tumor for EF depletion (Fig 2.7B).

I instead turned to A673 AID cells as an alternative for in vivo depletion of EF. As described above, I implanted A673 AID^{TIR1} cells in six NSG mice resulting in palpable tumors. I treated mice with either a 200mpk IAA formulation or vehicle twice a day and sacrificed mice after 2 or 4 total doses. At the time of sacrifice, I collected tumor and plasma samples. Western blot showed EF depletion after 24h of IAA dosing and almost no detectable EF levels in tumor treated for 48h (Fig 2.7C). Since IAA treatment showed in vivo EF depletion, a trial to measure changes in tumor volume following EF depletion was established. 14 NSG mice were injected with A673 AID^{TIR1} cells and monitored for tumor growth. 18 days after implantation, mice were treated with either 200mpk IAA or vehicle IP injections twice a day. Over the resulting 4 days, there was a decrease in tumor size in all IAA treated tumors with continued growth for vehicle treated tumor (Fig 2.7D).

Based on the promising EF depletion and tumor size reduction seen in pilot experiments with IAA treatment, a long-term tumor volume experiment with two cohorts of NGS mice injected with either A673 AID^{TIR1} or A673 AID^{only} cells to form xenografts was established. A673 AID^{only} cells were not transduced with the TIR1 expression construct and were used to ensure that any tumor size changes are due to TIR1 mediated depletion of EF and not other off-target effects of IAA injections. Tumor volumes in both cohorts were followed from implantation until sacrifice. 18 days following implantation, all mice in both cohorts had sizeable tumors and were treated every 12 hours with either IP 200mpk IAA or vehicle. Mice in both cohorts were treated until vehicle treated mice met the criteria for euthanasia, a total of 11 days. A subset of vehicle and IAA treated mice in the A673 AID^{TIR1} cohort were sacrificed at 2 days (D2) or 4 days (D4) following the start of dosing to track initial changes EF protein levels. As seen in prior experiments, mice treated with IAA in the A673 AID^{TIR1} cohort had an initial decrease in tumor volume but resumption of tumor growth after 4 days of treatment (Fig 2.7A, D). Meanwhile IAA tumors in the A673 AID^{only} cohort had no change in tumor volume across treatment groups (Fig 2.7B).

To determine the cause of the decrease and subsequent rebound in tumor size volume in the A673 AID^{TIR1} group, I examined EF protein levels in xenograft lysates collected from mice sacrificed at 2,4, or 11 days (D2, D4, or D11) after the start of treatments. Tumor samples obtained from vehicle or IAA treated mice on D2 showed depletion of EF in the IAA treatment condition. However, samples collected at D4 showed almost no difference in EF levels between treatment groups (Fig 2.7C). Similarly, EF levels in tumors from mice

sacrificed at the end point showed no discernable EF levels between vehicle and IAA treated samples (Fig 2.7E).

Since IAA mediated EF depletion is dependent on IAA treatment as well as TIR1 expression, I checked the level of expression of TIR1 in the tumor harvested in later time points. As compared the D2 IAA treated samples, which had shown induced EF depletion, the D11 IAA treated samples showed much lower levels of TIR1 expression (Fig 2.7E). To ensure that TIR1 loss was due to selective pressure by IAA treatment and not a result of a general growth advantage, I compared levels of TIR1 in D11 vehicle treated xenografts with D11 IAA treated xenografts. TIR1 levels in the vehicle treated tumor were higher than the TIR1 levels in IAA treated tumors (Fig 2.7F). This data suggests that the poor EF depletion and corresponding increase in tumor volume is due to the selection of a low TIR1 population that is no longer sensitive to IAA mediated degradation.

Table 2.1: List of validated inducible degron Ewing cell lines

Cell Line	Degron	Resistance	Spacer	Epitope Tag
A673	SMASh	Neomycin	GSSTGSG	3xFLAG
A673	SMASh	Neomycin	PGP	V5
A673	SMASh	Neomycin	PGP	Untagged
A673	AID	Neomycin	PPG	3xFLAG
A673	AID	Neomycin	PPG	Untagged
TC32	SMASh	Neomycin	PPG	Untagged
TC32	SMASh	Neomycin	GSG	Untagged
SKNMC	SMASh	Neomycin	PPG	Untagged
SKNMC	SMASh	Neomycin	GSG	Untagged

Table 2.2: Significant transcript changes after EF depletion

Cell Line	Timepoint	Downregulated Genes	Upregulated Genes
A673 SMASh	6h	52	32
A673 SMASh	12h	180	188
A673 SMASh	24h	558	984
A673 SMASh	24h	744	1679
TC32 SMASh	24h	1016	1148
SK.N.MC SMASh	24h	885	1201

Table 2.3: FPKM changes in following EF depletion in known EF target genes

Upregulated Genes	TC32 SMASh		SK.N.MC SMASh		A673 SMASh	
	DMSO	Danoprevir	DMSO	Danoprevir	DMSO	Danoprevir
IGFBP5	28.322	135.034	11.266	93.470	3.238	277.4036
DKK1	0.920	93.709	0.088	0.178	3.675	385.372
CDKN1C	5.820	65.398	0.672	4.453	0.970	4.414
DKK3	2.194	6.35	0.277	6.309	2.371	30.461

Downregulated Genes	TC32 SMASh		SK.N.MC SMASh		A673 SMASh	
	DMSO	Danoprevir	DMSO	Danoprevir	DMSO	Danoprevir
CCND1	360.749	27.581	659.548	74.172	621.616	50.852
NKX2.2	100.025	33.759	46.0108	19.033	53.297	19.951
MYC	130.201	38.132	232.466	11.971	67.274	23.975
NR0B1	304.338	4.979	20.204	1.561	9.361	1.976

Figure 2.1

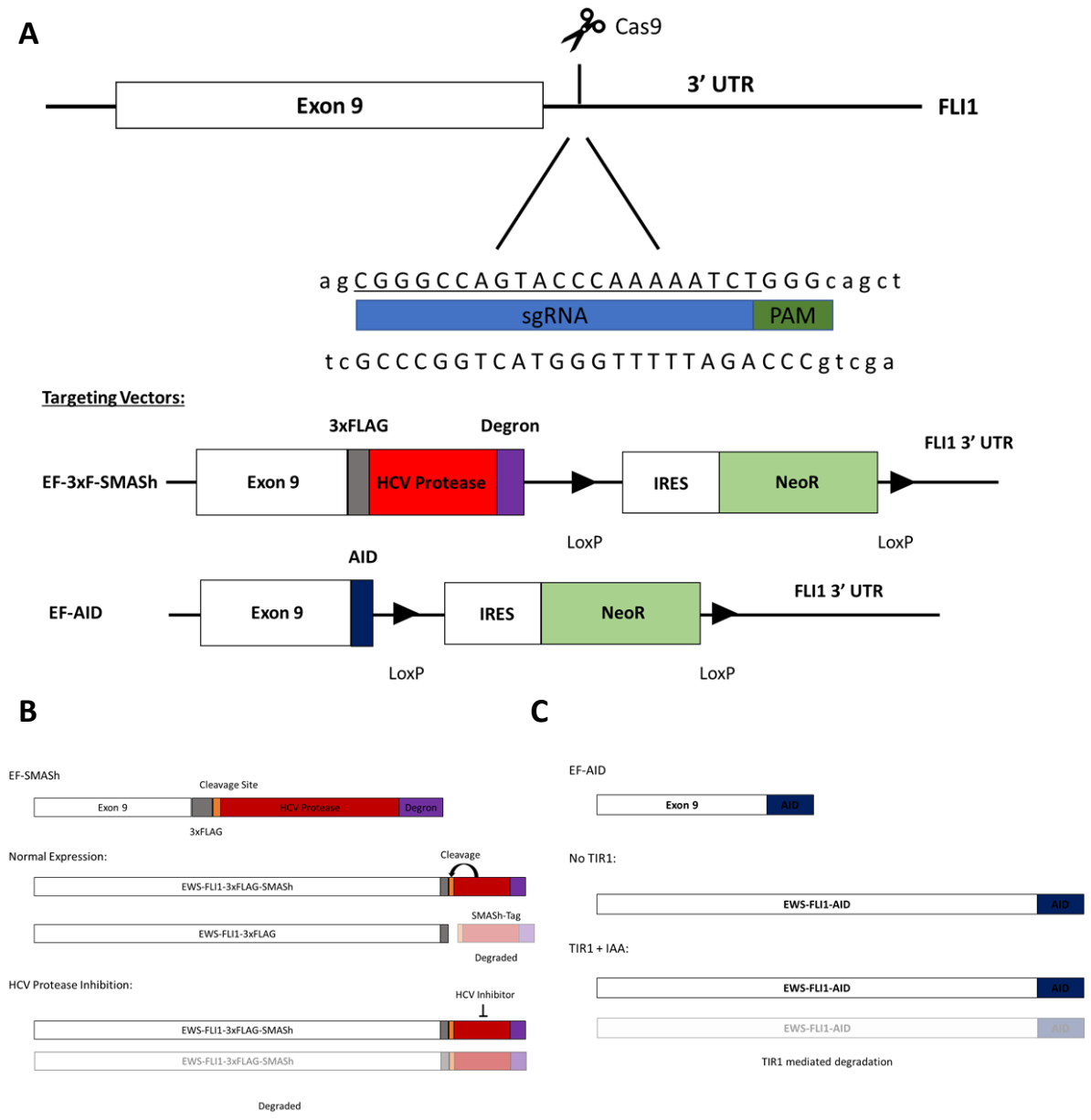

Figure 2.1: Targeting Endogenous EF with degron systems. (A) Diagram depicting the targeting strategy for introduction of SMASh and AID tags into the 3' end of the endogenous FLI1 locus. (B) Diagram of EF-SMASh system showing expected protein expression and degradation under +/- Danoprevir treatment. (C) Diagram of EF-AID system showing expected expression and degradation in the presence of AID +/- TIR1.

Figure 2.2

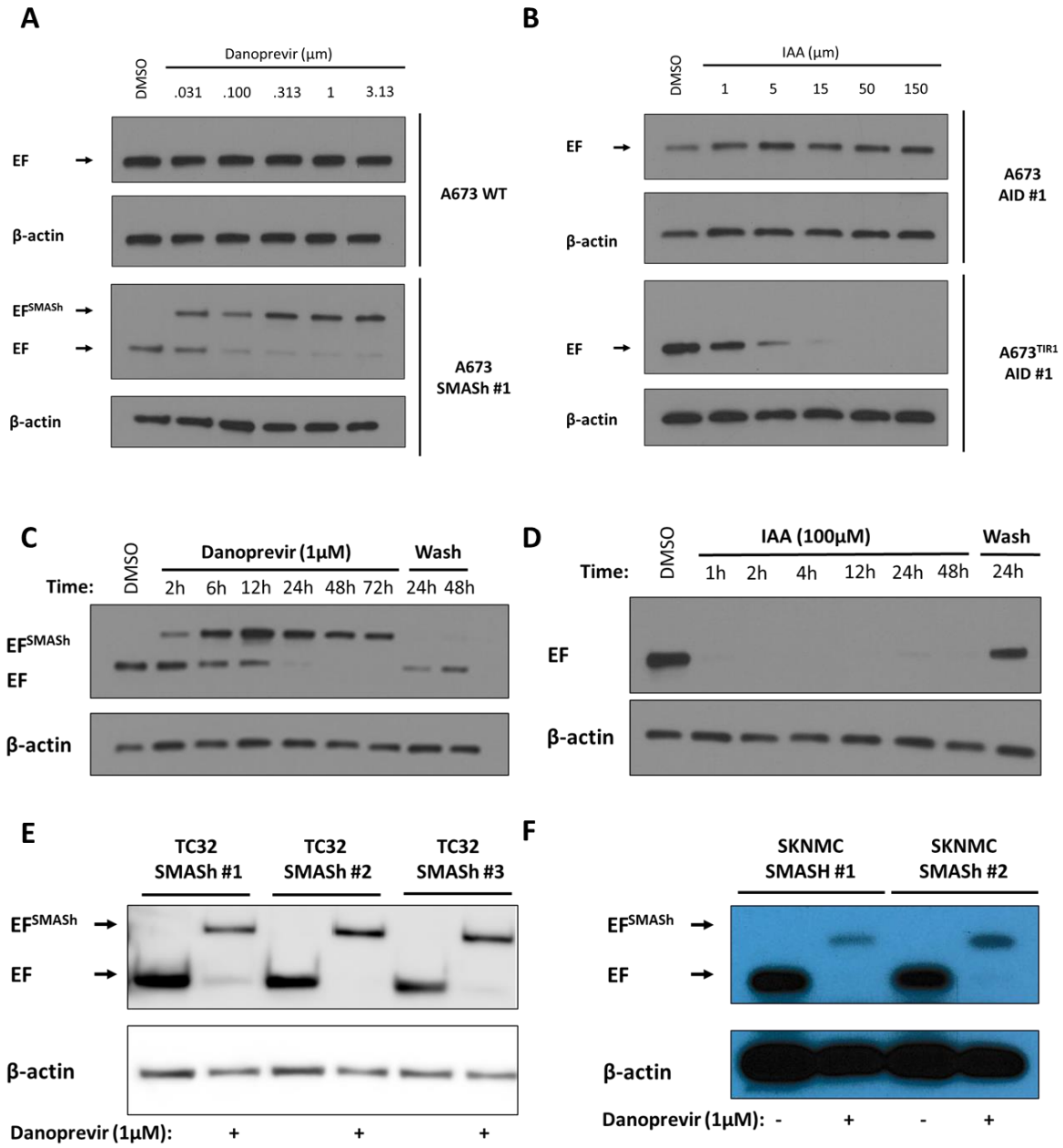

Figure 2.2: Depletion of EWS-FLI1 with inducible degron system. (A) Lysates of A673 WT or A673 SMASh #1 clones treated with increasing Danoprevir dosed over 24h period were immunoblotted for FLI1. (B) Immunoblot for FLI1 of A673 AID #1 clones with or without TIR1 and treated with increasing doses of IAA over a 24h period. Immunoblot of A673 SMASh (C) or AID (D) clones during treatment time course. Immunoblot of TC32 (E) or SK.N.MC (F) SMASh clones with or without Danoprevir.

Figure 2.3

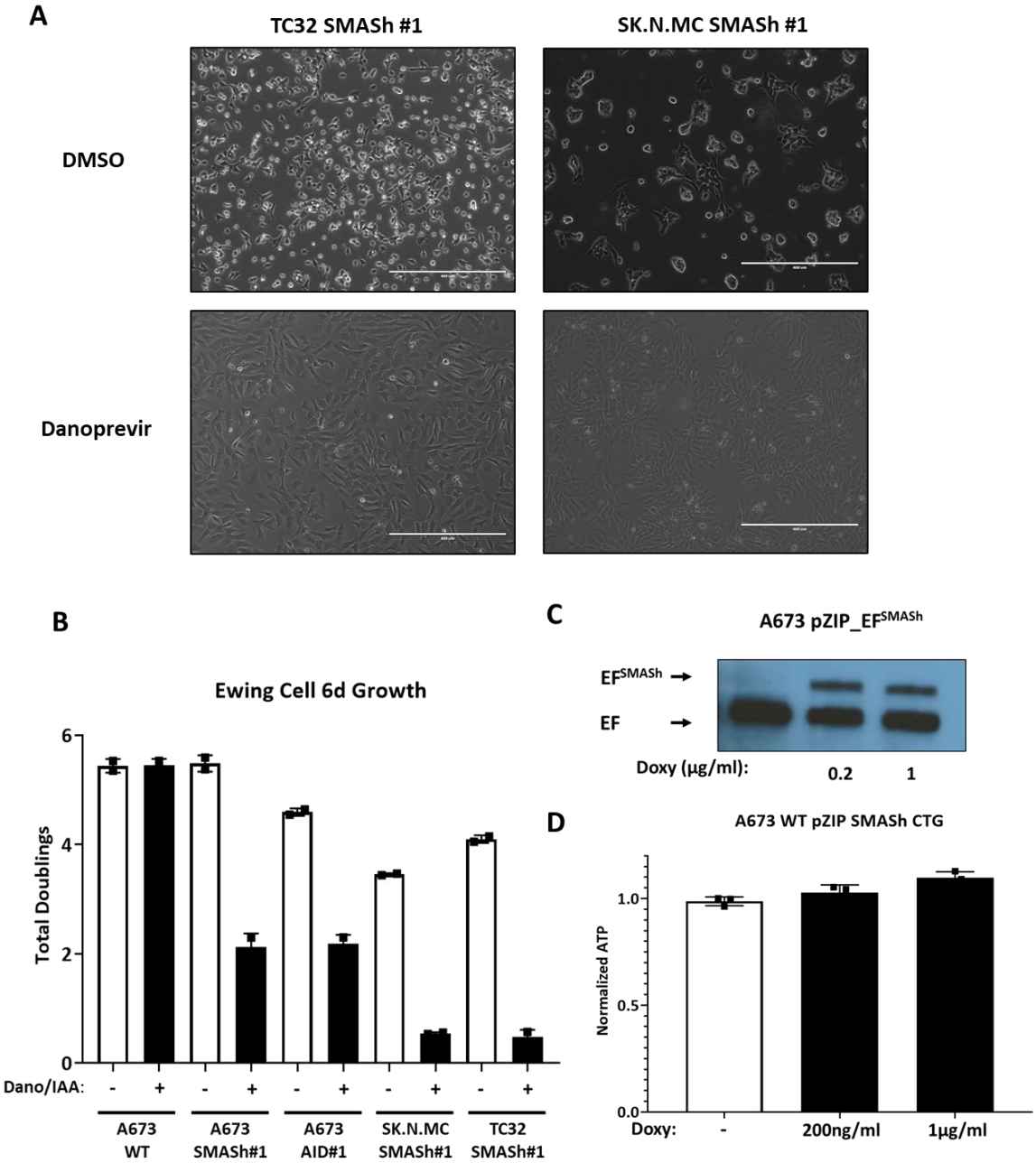

Figure 2.3: EF depletion causes proliferation defects and expression EF^{SMASh} has no effect on proliferation. (A) Bright field images showing TC32 and SK.N.MC cells treated with +/- Danoprevir for 48h. (B) Total doublings of Ewing cell lines after 6 days on +/- Danoprevir (C) immunoblot showing A673 WT cells with induced EF^{SMASh} expression. (D) Normalized ATP after inducing expression of EF^{SMASh} in A673 cells for 5 days.

Figure 2.4

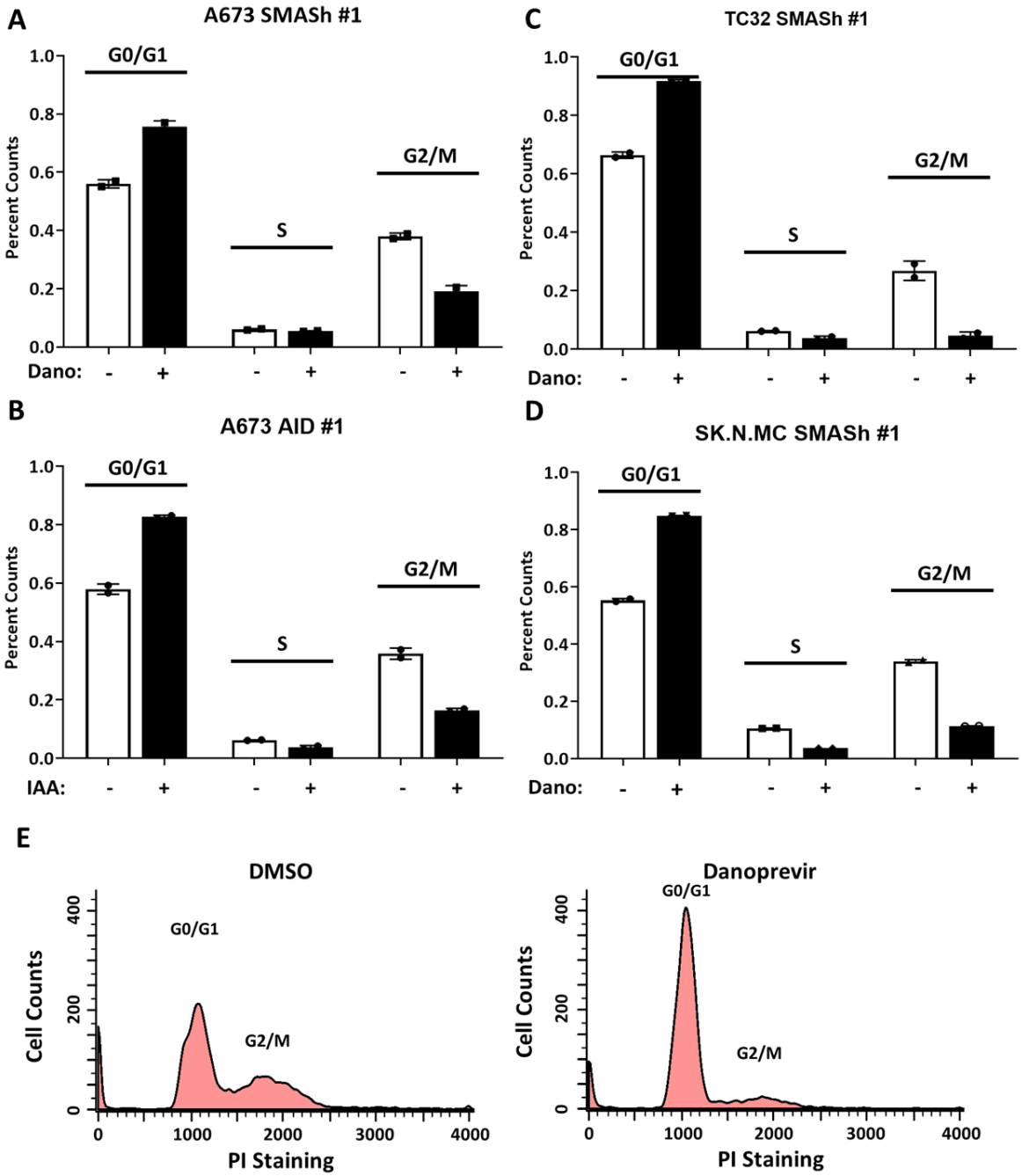

. **Figure 2.4: EWS-FLI1 depletion leads to G1/S arrest.** (A-D) Distribution of PI stained cells counted in flow cytometry analysis of A673 SMASh (A) , A673 AID (B), TC32 SMASh #1 (C), or SK.N.MC SMASh (D) cells with 24h of treatment in gated groups: G0/G1, S, G2/M. (E) Cell cycle tracing of SK.N.MC SMASh#1 clone after 24h of +/- Danoprevir treatment.

Figure 2.5

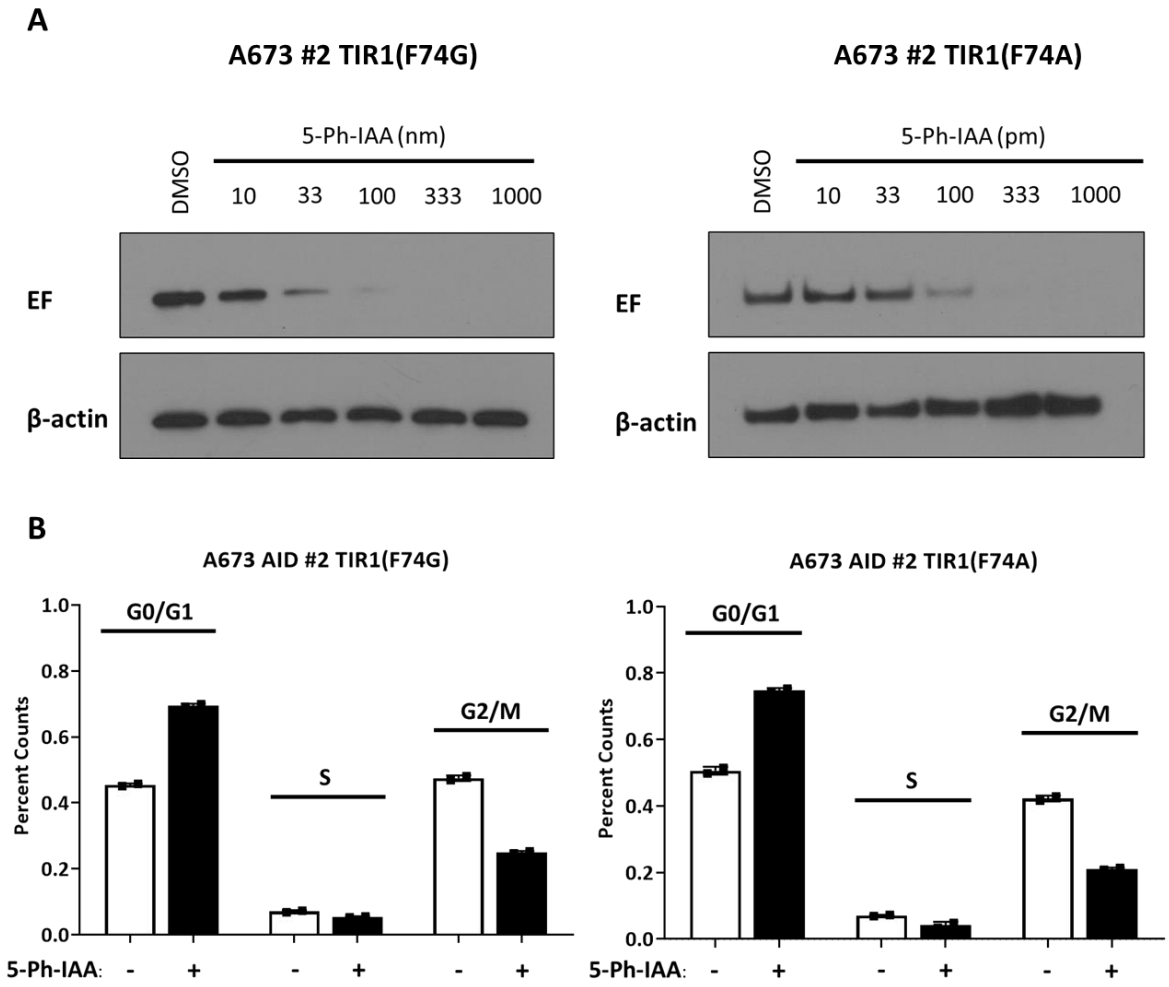

<u>Figure 2.5</u>: AID 2 System increases depletion sensitivity to 5-Ph_IAA. (A) FLI1 immunoblot of A673 #2 lysates showing EF depletion with increasing doses of 5-Ph-IAA. (B) Distribution of PI stained A673 #2 AID cells in different cell cycle phases after 24h of +/- 5-Ph-IAA treatment.

Figure 2.6

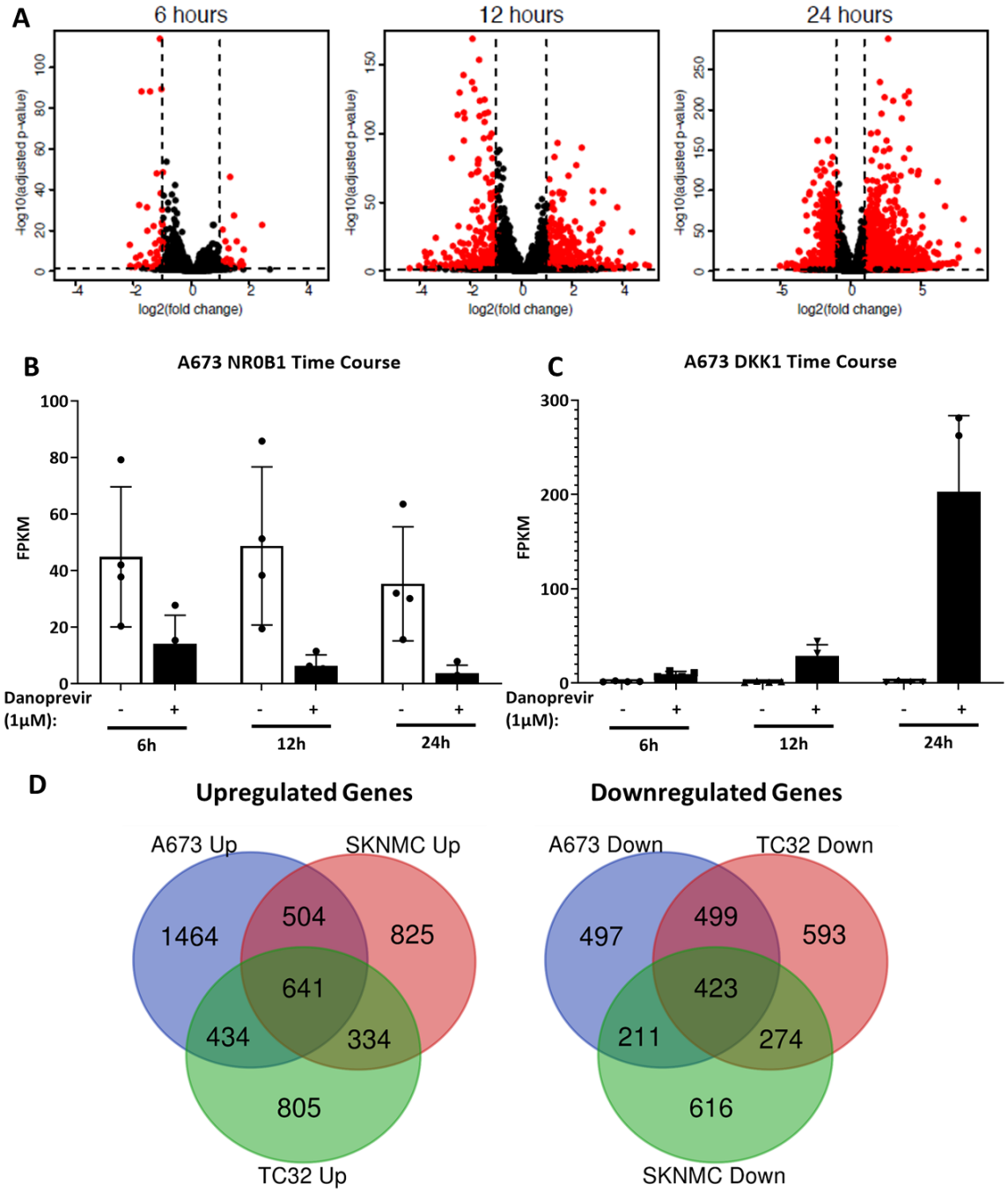

Figure 2.6: Depletion of EWS-FLI1 leads to upregulated and downregulated transcripts. (A) Volcano plot showing transcript changes in A673 SMASh clones at 6,12,24h after Danoprevir treatment. FPKM changes in A673 SMASh clones of NR0B1 (B) or DKK1 (C) after Danoprevir treatment. (D) Venn diagram showing common transcript change between different SMASh Ewing cell lines at 24h after Danoprevir treatment.

Figure 2.7

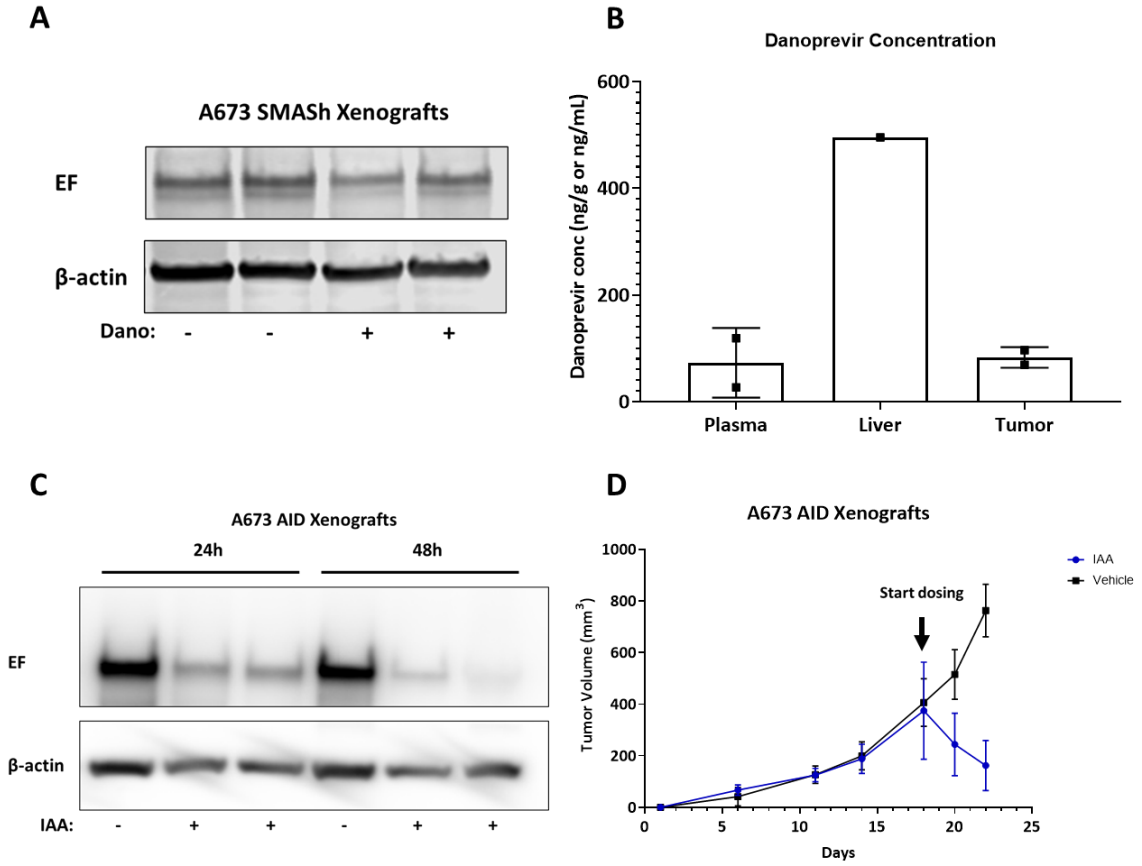

<u>Figure 2.7</u>: In vivo IAA treatment depletes EF and decreases tumor volume. (A) FLI1 immunoblot of A673 SMASh xenografts after 48h of BID +/- 30mpk Danoprevir treatment. (B) Concentration of Danoprevir in plasma, liver, and tumor of treated mice. (C) Immunoblot of xenograft lysates after 24 or 48h of +/- 200mpk IAA treatment. (D) Tumor volumes of 10 IAA treated mice and 4 vehicle treated mice from implantation until sacrifice. Start of BID dosing on day 18.

Figure 2.8

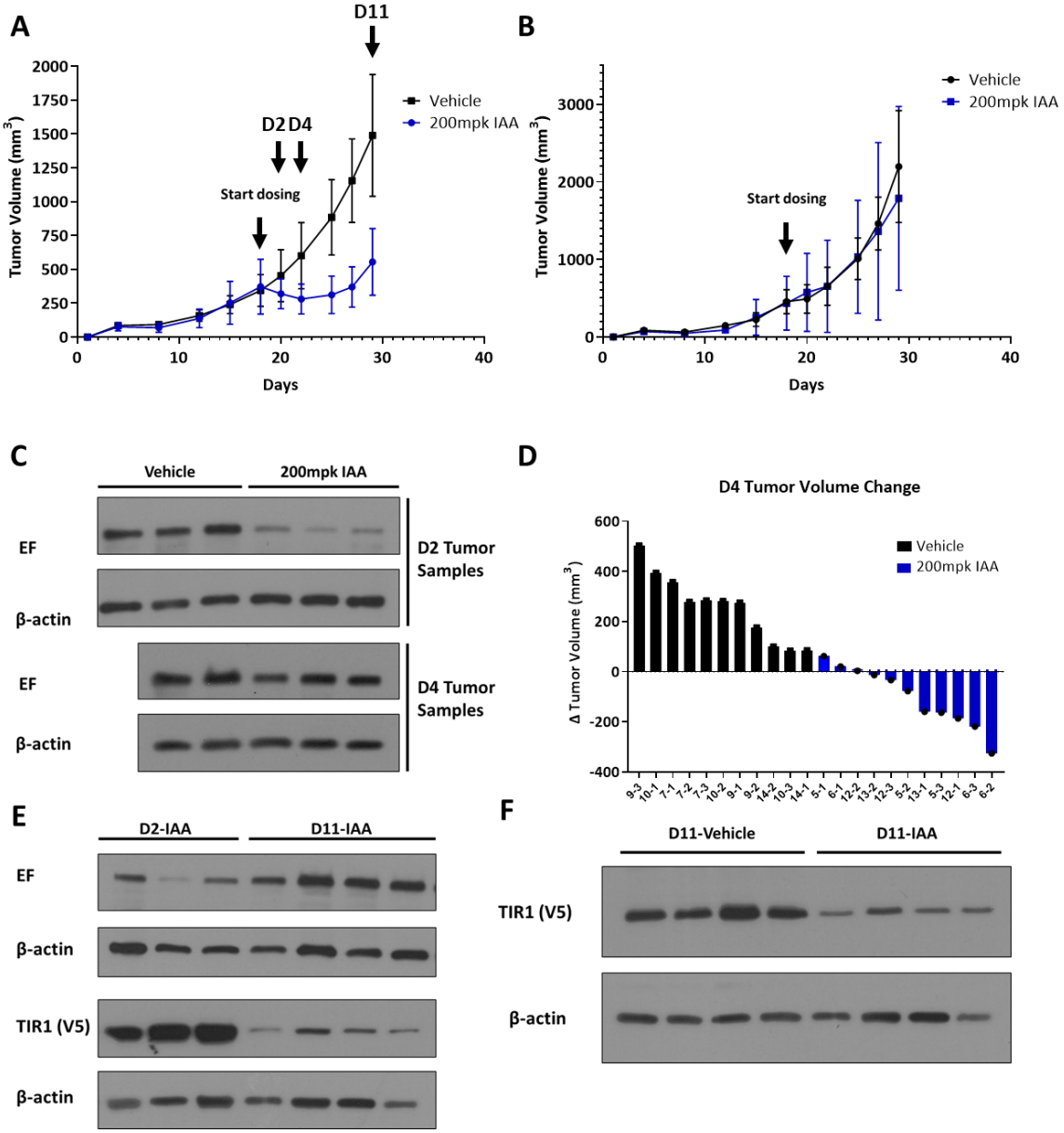

Figure 2.8. In-vivo depletion of EF depletion is dependent on TIR1 expression. (A) Curve of tumor size for A673 $^{AID+TIR1}$ xenografts from implantation (Day 0) with start of dosing at day 18, and dates of sacrifice denoted by arrows. (B) Curve of tumor size for A673 AID ^{only} xenografts. (C) Immunoblot of FLI1 showing lysates from xenograft obtained on D2, D4 treated with vehicle or IAA. (D) Change in individual xenograft volume from start of IP dosing (Day 18) to D4 (Day 22). (E) Immunoblot of FLI1 and V5 of xenograft treated with 200mpk IAA and harvested on either D2 or D11. (F) Immunoblot of V5 (TIR1) of D11 xenografts treated with either vehicle or IAA.

CHAPTER THREE
N-Terminus of EWS Contains Redundant Peptide Repeats That Are Necessary for Ewing Sarcoma Proliferation

3.1 Re-expression of EWS-FLI1, but not Cyclin D1 rescues proliferation in Ewing sarcoma cells

During the characterization of the EF degrons, I saw that washout of drug media allowed for re-expression of endogenous EF (Fig 2.2C, D). I tested to see if continued passaging of SMASh cells after withdrawal of Danoprevir would restore proliferation. I passaged TC32 WT, which have no degron system, and a TC32 SMASh clone on Danoprevir or vehicle for 3 days and the preformed a media wash. I allowed cells to continue growing for 6 days after washout. While proliferation was temporarily inhibited, EF depleted SMASh cells began to proliferate as normal 3 days after washout (Fig 3.1A). This return to normal proliferation demonstrates that G1/S arrest and decrease proliferation phenotype is dependent of EF expression levels and reversible. These results contradict prior studies that have described the EF depletion phenotype as senescent and reiterate the importance of EF as a proliferative signal in Ewing cell lines.

A key regulator of the G1/S transition that is altered by EF depletion is cyclin D1. In both the A673 time-course RNA seq data and the Ewing cell line RNA seq, cyclin D1 levels were greatly reduced after EF depletion (Table 3). Since G1/S arrest is a consistent feature of EF depletion, I sought to re-express cyclin D1 to see if that would be sufficient to cause Ewing cell proliferation in the setting of EF depletion. I utilized the CRISPR/Cas9 synergistic

activation mediator (SAM) system (49) as a way of increasing cyclin D1 expression in Ewing cell lines. This system uses sgRNA targeted dCas9-VP64 alongside MS2-P65-HSF1 (MPH) effectors to increase transcription of a selected target gene via a guide RNA (49). I transduced TC32 SMASh cells with the MS2-P65-HSF1 effector system and subsequently transduced with the LentiSAMv2 containing dCas9 and either a non-targeting control sgRNA or three sgRNA's targeting cyclin D1, which I called TC32 SAM. I checked expression level of cyclin d1 in with or without depleted EF for cells transduced with all guides. TC32 SAM cells expressing the non-targeting guide had a dramatic drop in cyclin D1 protein level after EF depletion (Fig 3.1B). TC32 SAM cells expressing any of the 3 guides targeting, cyclin D1 had near endogenous levels of cyclin D1 after EF depletion (Fig 3.1B).

I then checked if CRISPR SAM driven re-expression of cyclin D1 levels were sufficient to overcome the G1/S arrest and proliferation defects seen with EF depletion. I treated TC32 SAM cells expressing either a control guide or a guide targeting with Danoprevir for 48h and fixed cells for PI staining. TC32 SAM cells with guides targeting cyclin D1 still had an increase in percentage of cells in G1 after endogenous EF depletion (Fig 3.1C). Additionally, a 5-day proliferation assay of TC32 SAM cells with either a control or cyclin D1 guides showed limited proliferation in the setting of EF depletion (Fig 3.1D). Together these findings indicate that re-expression of cyclin D1 alone is insufficient to reverse the proliferative changes caused by EF depletion in Ewing cells.

3.2 Expression of EWS-FLI1 in Ewing sarcoma cells rescues cell cycle arrest

Since prior studies and my data both indicate that EF is a primary driver of proliferation, I built a system to rescue proliferation defects by expressing exogenous EF during endogenous EF depletion. Using a CMV driven promoter, I made a lentiviral constitutive expression system of EF. I selected SK.N.MC and TC32 SMASh clones for transduction with the expression system for EF or an empty vector, hereto referred to as SK.N.MC or TC32-EF or Empty. I validated exogenous EF expression in TC32-EF cells in the presence or absence of endogenous EF depletion (Fig 3.2A). I then tested the ability of both TC32-EF and Empty cells to proliferate with or without endogenous EF. I passaged each cell line on vehicle and Danoprevir media over a 12-day period. TC-Empty with depleted endogenous EF showed limited proliferation over the entire assay period, however TC32-EF cells with depleted endogenous EF were able continue growing at comparable levels to that of vehicle treated cells (Fig 3.1B).

Next, I analyzed the cell cycle status of TC32-EF and Empty cells treated with or without Danoprevir. As seen by the differences in proliferation, TC32-Empty cells with depleted endogenous EF accumulated in the G1/S phase, while TC32-EF cells showed minimal changes to cell cycle status (Fig 3.1D). I then isolated RNA from TC32-EF & Empty cells 24h after Danoprevir or vehicle treatment. Using quantitative PCR (qPCR), I checked the expression of NR0B1 and DKK1 after endogenous EF depletion in both TC32-EF and Empty cells through qPCR to see if the transcript changes seen in my RNA seq data following EF depletion were ameliorated by exogenous EF expression. TC32-EF cells had DKK1

expressions levels near those of vehicle treated cells after endogenous EF depletion. Meanwhile, TC-Empty cells saw an almost 100-fold drop in DKK1 expression levels after EF depletion (Fig 3.2C). Constitutive exogenous EF in TC32-EF cells also limited the rise in NR0B1 expression level after Danoprevir treatment as compared to treated TC32-Empty cells (Fig3.2C). Across proliferation, cell cycle status, and EF dependent transcripts, exogenous EF expression was able to functionally substitute for endogenous EF.

3.3 Exons in the N-terminus of EF are redundant for Ewing sarcoma cell proliferation

The data gathered from EF degron systems demonstrate that proliferation is a robust and sensitive readout of EF function in Ewing cell lines and xenografts. With the pLVX expression system described above, I have a tool to introduce exogenous EF variants in the setting of endogenous EF depletion. Together these tools can be combined to form a proliferation-based assay to determine the necessary and sufficient portions of EWS required for EF function. By constitutively expressing a truncated or mutant EF construct in a Ewing cell line and serially passing those cells while depleting endogenous EF depletion, I can assess the role of the altered portion on proliferation. Due to their sensitivity to EF loss, I chose the TC32 and SK.N.MC SMASh clones as biological replicates to test the capacity of a series of EWS variants to drive proliferation absent endogenous EF.

To probe if any region within EWS contains necessary elements for Ewing cell proliferation, I built a series of EF constructs without each exon of EWS. To ensure I was comparing truncations of similar size, I treated exon 1&2 as a pair in these experiments. I transduced

SK.N.MC and TC32 SMASh clones and tittered expression of these truncated EF variants to match expression levels of endogenous EF protein. After validating expression, I passaged these cells in 3-day increments for a total 12-day period maintaining them on either Danoprevir or vehicle media for the duration of the assay (Fig 3.3A). The time scale of this assay was selected to ensure that any exogenous EF variant was able to drive sustained long-term proliferation. Surprisingly, expression of any EF construct with a single exon deletion was sufficient to drive TC32 or SK.N.MC cell proliferation in the setting of endogenous EF depletion (Fig 3.3B). Had an individual exon contained an essential domain for proliferation, I would have expected to see a lack of proliferation over the assay period. However, the continued proliferation of all constructs in this experiment argues that portions of the N-terminal region of EWS can compensate for the loss of other regions and maintain proliferative signaling when a single exon is deleted.

Given that portions of the N-terminus of EWS are functionally redundant, I made a series of EF variants with cumulative exon deletions starting from either the N or C terminus of the EWS portion to identify a minimal portion required for proliferation. Starting from the N terminus, deletion of exons 1-4, a loss of 75 amino acids, resulted in an EF variant that was no longer able to rescue proliferation under the setting of endogenous depletion. Incremental exon deletions starting from the C-terminus showed that loss of exons 5-7, a 189 amino acid deletion, resulted in EF variants that had minimal or no ability to rescue proliferation (Fig 3.3C). This data suggest that proliferation is more sensitive to N-terminal deletions than C-terminus since the Δ1-4 construct is only a 75 amino acid deletion, while the Δ5-7 is a 189

amino acid deletion. This data matches previous reports where loss of either the N or C portion of the EWS translocation portion allowed for transcriptional activity in a transcriptional reporter assay or induced EF-like transcriptional fingerprint in MSC (43, 44).

3.4 Exons in the N-terminus of EF are redundant for Ewing sarcoma proliferation

Previous studies (43, 44) have shown that tyrosines within the N-terminal region of EWS are required for EF transcriptional activity. Given that loss of exons 1-4 was sufficient to prevent proliferation rescue, I created a series of tyrosine mutants in the first four exons of EWS to see if they are uniquely necessary for proliferation. As in the experiments above, SK.N.MC cells and TC32 cells were transduced and subsequently passaged for 12 days on either Danoprevir or vehicle. Mutation of tyrosines to serines in any individual exon did not affect the ability of EF variants to rescue proliferation. Much like my finding in the truncation constructs perturbation of exons 1-3 either through deletion or mutation of tyrosine to serine rescued proliferation while deletion or tyrosine to serine mutation across exons 1-4 resulted in non-proliferative EF variants (Fig 3.3B).

Prior transcriptional studies have found that tyrosine to phenylalanine mutations can recapitulate the transcriptional activation of EF (43). I mutated all 13 tyrosines in exon 1-4 of EF to phenylalanine and expressed the construct in SK.N.MC and TC32 cells. After serially passing these cells over a 12 day period, the YF(1-4) mutant able to continue proliferating despite endogenous EF depletion (Fig 3.3B). These results indicate a necessity for the aryl rings in the EWS portion for Ewing cell proliferation.

Based on my tyrosine and deletion results, I hypothesize that there exists tyrosine redundancy throughout the first seven exons of EWS. To identify which tyrosines are redundant in the first four exons, I made a series of tyrosine mutants of the EF variant Δ6,7. A described above, I expressed these constructs in TC32 and SK.N.MC cells and tested their ability to rescue proliferation in the context of EF depletion. With the loss of a large set of tyrosines at the C-terminal end EWS, mutation of at least 3 tyrosines to serines in the N terminal portion resulted in a functionally dead variant (Fig 3.3C). These data are a strong indication of redundancy of tyrosine throughout the N-terminus of EWS. There appears to be functional floor for EF with at least 11 tyrosines as seen by the limited but continued proliferation of the YS (1-2) Δ6,7 construct.

3.5 FUS-ETS Translocations do not rescue proliferation of EWS-ETS Ewing driven cell lines.

Since there have been more detail structural studies of the LC domain of FUS, including fine mapping of the functional tyrosines and a proposed structure to the core of CL fibrils (40-41), FUS may function as basis for understanding key structural elements in the LC of EWS. Since there are reports of FUS involved in some Ewing sarcoma tumors (8), I tested to see if FUS containing translocation would be able to substitute for EWS in EF driven cell lines. I built a series of FUS expressing constructs that contained the first seven exons of FUS, since these are contained in previously described FUS-ERG driven Ewing sarcoma tumors and contain the LC domain (8). To ensure that EWS and FUS translocation functional

discrepancies were not due to the ETS partner in the translocation, I built a constitutive expression vector for FUS-FLI1 (FF), FUS-ERG (FE), and EWS-ERG (EE).

I transduced SK.N.MC SMASh cells with pLVX expression vectors for EWS and FUS translocation and matched protein expression of these constructs to that of endogenous EF. I then passed these cells every 3 days on vehicle or Danoprevir in a 12-day proliferation assay. EWS translocations involving either ERG or FLI1 were able to maintain proliferation in the setting of endogenous EF depletion (Fig 3.4B). However, both FF and FE expressing cells stopped proliferating after 6 days (Fig 3.4A, B). At the end of the 12-day assay only EF and EE were able to drive proliferation, suggesting that FUS and EWS may not be functionally interchangeable in Ewing cell lines.

Figure 3.1

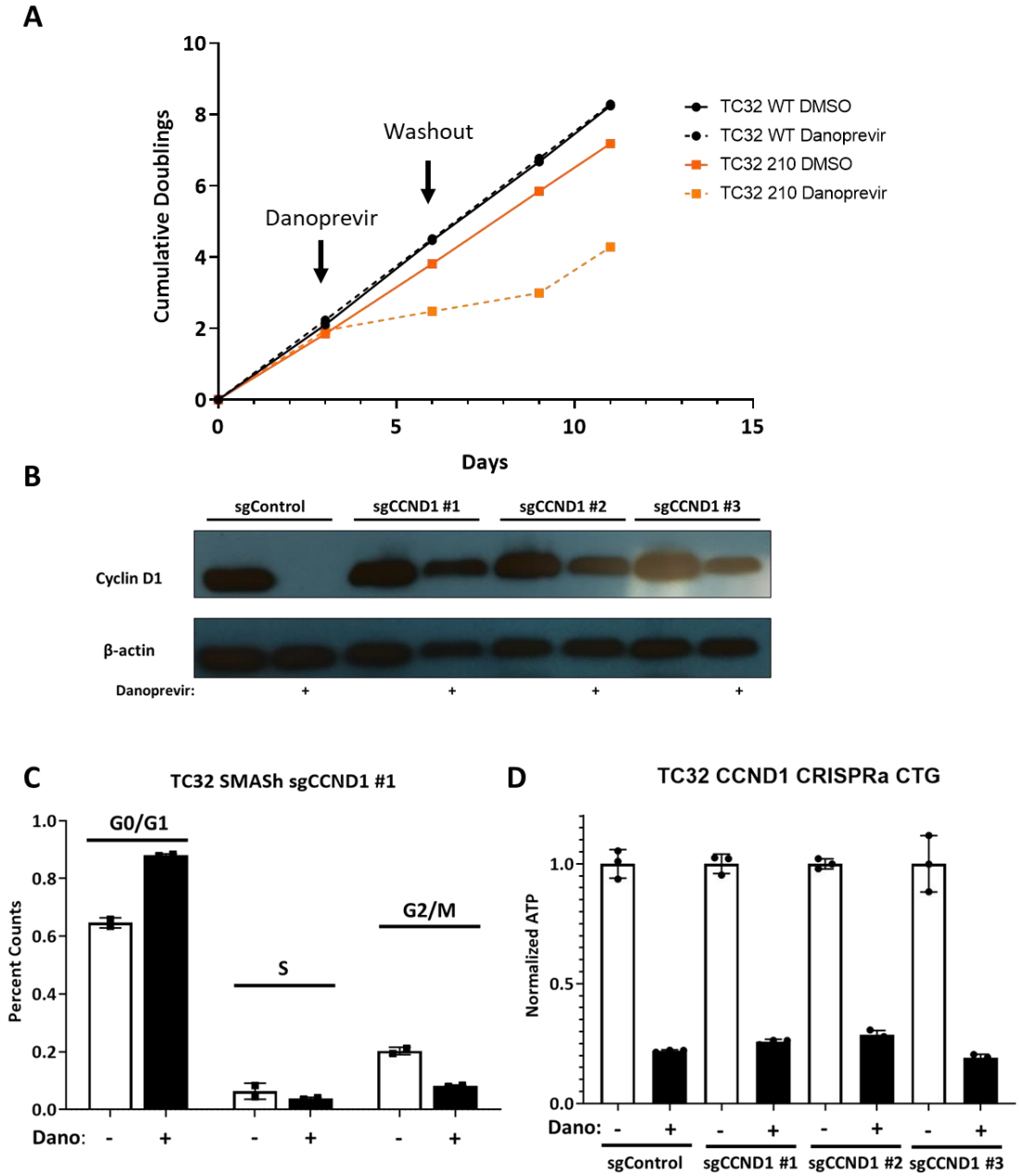

Figure 3.1: Re-expression of EF, but not Cyclin D1 is sufficient to rescue proliferation in Ewing cell lines. (A) Cumulative doublings of TC32 WT or SMASh after 3-day dose of Danoprevir (day 3-6) and subsequent washout (day 6-12). (B) Immunoblot of cell lysates of TC32 SMASh cells with CRISPRa and 3 sgRNA for Cyclin D1. (C) Normalized counts of PI stained TC32 SMASh cells with sgControl or sgCCND1 +/- Danoprevir for 48h. (D) Normalized ATP via cell titer glow of TC32 SMASh cells with CRISPRa guides for CCND1 +/- Danoprevir.

Figure 3.2

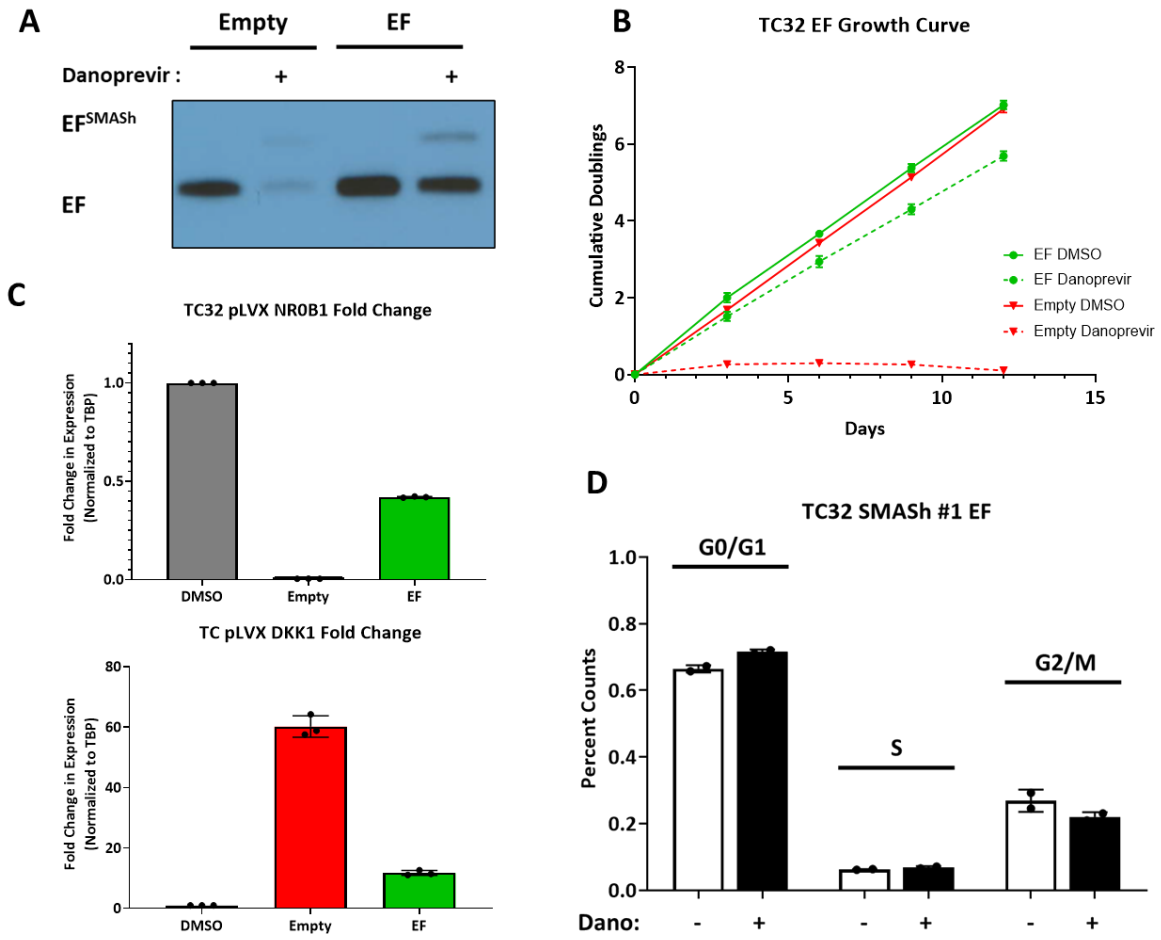

Figure 3.2: Re-expression of EF rescues proliferation & gene expression. (A) Immunoblot for FLI1 of TC32 SMASh #1 cells transduced with either empty vector or vector expressing exogenous EWS-FLI1 after 24h of +/- Danoprevir. (B) Growth curves of TC32 SMASh-EF or Empty cells that have been serially passaged on DMSO or Danoprevir media. (C) Fold change in expression of NR0B1 and DKK1 between TC32 SMASh Empty DMSO and Empty or EF cells treated with Danoprevir for 24h. (D) Distribution of PI-stained cells in flow cytometry analysis of TC32 SMASh-EF cells after 24h of DMSO or Danoprevir treatment.

Figure 3.3

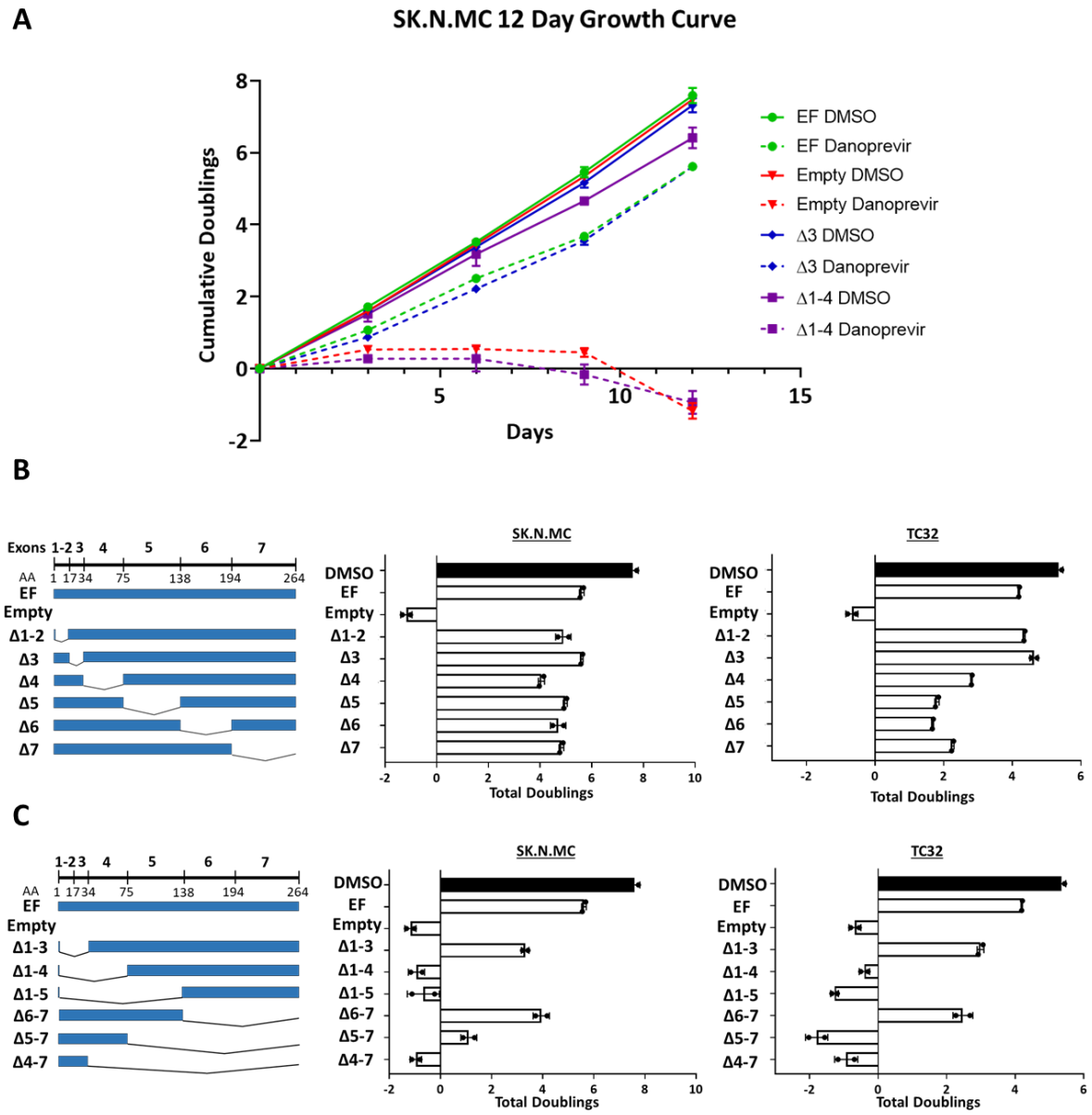

Figure 3.3: Individual exons in EWS are redundant for ES proliferation. (A) Growth curve showing cumulative doublings of SK.N.MC cells transduced with a series of transduced EF constructs: EF, Empty, Δ3, or Δ1-4 and serially passaged on either DMSO (solid lines) or Danoprevir (dotted lines) for 12 days. (B-C) Summary of total doublings for single exon (B) or larger (C) EF truncation construct expressed in SK.N.MC or TC32 cells after 12-day growth assay.

Figure 3.4

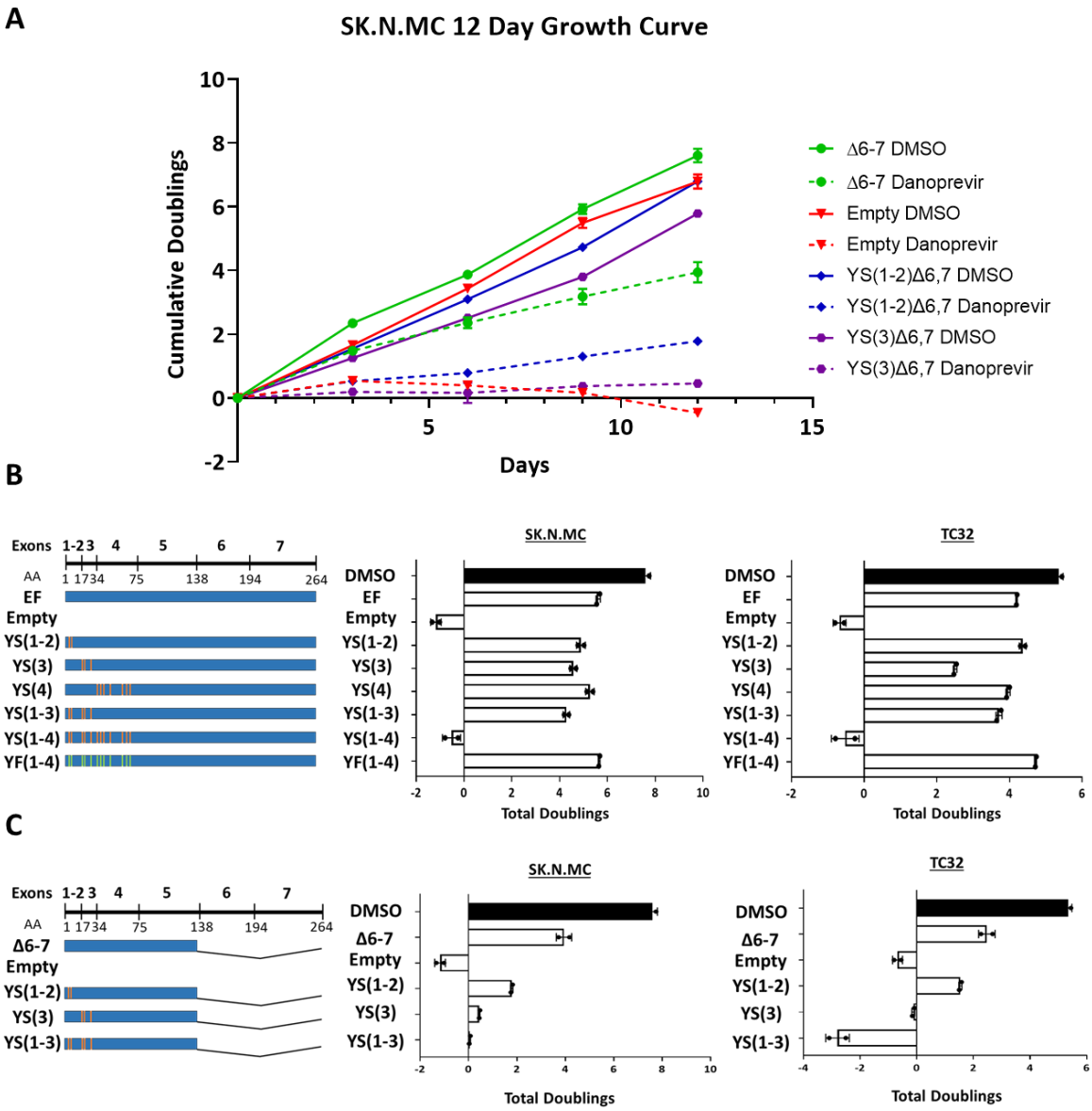

Figure 3.4: **Tyrosine residues are redundant, but necessary for EF proliferation.** (A) Growth curve showing cumulative doublings of SK.N.MC cells transduced with a series of transduced EF constructs: Δ6-7, Empty, YS(1-2) Δ6,7, or YS(3)Δ6,7 and serially passaged on either DMSO (solid lines) or Danoprevir (dotted lines) for 12 days. (B-C) Summary of total doublings for single exon tyrosine to serine mutations (B) or (C) N-terminal tyrosine to serine mutations in EF truncation constructs expressed in SK.N.MC or TC32 cells after 12- day growth assay.

Figure 3.5

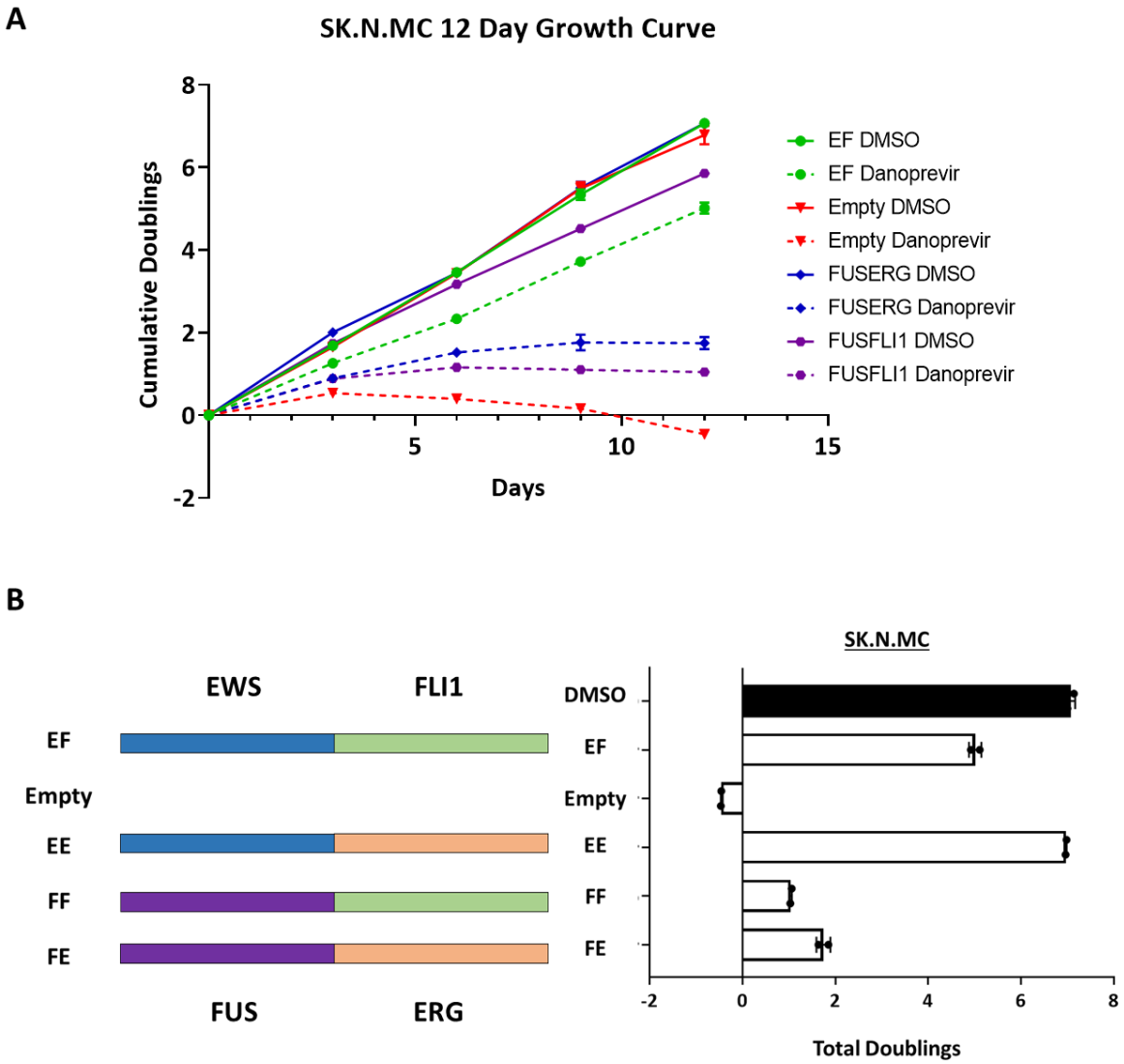

Figure 3.5: FUS-ETS Translocations are unable to rescue proliferation arrest after EF depletion. (A) Growth curve showing cumulative doublings of SK.N.MC cells transduced with either EWS-ETS or FUS-ETS constructs. (B) Diagram showing EWS-ETS and FUS-ETS constructs as well as the total doublings counted after 12-day growth assay for each construct.

CHAPTER FOUR
Discussion and Conclusions

Discussion

Here I have described two distinct systems for inducible depletion of endogenous EF using degron tags. Targeting of the SMASh or AID tags to the endogenous locus of EF in a series of patient derived sarcoma Ewing cell lines allowed for EF depletion and a subsequently decreased proliferation through accumulation of cells in G1 phase of the cell cycle. The above work differs in strategy from previous studies that have relied on a variety of RNAi techniques to deplete EF in Ewing sarcoma cells (22-25). Off-target effects and incomplete EF knockdown that can result for siRNA techniques have made it difficult to make sense of the disparate reports of EF depletion phenotypes (22-25). The SMASh and AID systems avoid some of these issues by directly tagging a protein of interest for degradation. These systems were capable of reversible EF depletion that resulted in consistent proliferation, cell cycle, and transcriptional changes across multiple Ewing cell lines. The data gathered through my experiments helps provide a clearer consensus regarding the phenotype of EF depletion in Ewing cells. The reproducible accumulation of cells in the G1 phase after EF depletion across Ewing cell lines, including A673 cells, demonstrates a clear need for EF expression in cell proliferation. Meanwhile, the reversibility of these systems demonstrates that EF depletion does no cause permanent senescence. The importance of EF for growth in Ewing sarcoma is only underscored by the stark decreases in tumor size after EF depletion in vivo.

While there are clear advantages to inducible degrons, these systems also contain drawbacks such as the uncleaved SMASh product and the difficulties with targeting. Depletion of EF with the SMASh system results in the loss of endogenous EF and a detectable higher molecular weight species detectable with FLI1 or, when present in the SMASh tag, epitope tag immunoblotting. This higher molecular weight species matches the size of EF with the uncleaved SMASh system and has shift comparable to similar uncleaved SMASh products that were described in the characterization of the SMASh system (46). The presence of this band could be a potential confounder for studies of EF depletion. However, the consistency in cell cycle phenotype between A673 AID and SMASh depletion, it is likely that both degron systems can functionally deplete EF. An alternative concern about the presence of EF^{SMASh} if it is non-functional is that this species may be acting as a dominant negative and exaggerating the phenotype of depletion in SMASh samples. To test whether the higher molecular weight species was interfering with endogenous EF function or other aspects of proliferation, I expressed a version of EF^{SMASh} without the degron in A673 in the setting of endogenous EF and saw no proliferation defects. While some evidence described below from the results of endogenous EF targeting points to C-terminal tagging as deleterious for EF function, I'm unable to say that the EF^{SMASh} band is without function. Further studies examining SK.N.MC or TC32 SMASh cells passage with constitutive expression of the EF^{SMASh} are still required to see what if any effects this EF species has on continued proliferation after endogenous EF depletion.

Throughout my assays of proliferation, cell cycle, and even EF degron targeting, A673 have consistently shown a higher tolerance for EF functional defects. A673 cells appear to be less sensitive to C-terminal tagging of the endogenous EF. Throughout targeting attempts, multiple clones of A673 containing epitope or degron tags on the C-terminus of FLI1. However, I was only able obtain SK.N.MC and TC32 clones when the targeting strategy added no C-terminal tags or retained degron domains as in the case of the AID system (Table 1). As compared to other Ewing cell lines, A673 cells also appear to have a lower sensitivity to proliferation and cell cycle changes induced by EF depletion. Together these data suggest that A673 is less reliant of EF signaling to drive proliferation. This may be due to the additional proliferative signaling due to a V600E BRAF mutation. This MAP kinase activating mutation is not commonly found in Ewing sarcoma tumors and poses a potential confounding factor to studies of EF function in A673 cells. For this reason, I have used multiple Ewing cell lines to verify phenotypes observed initially in A673 cells.

Prior transcriptional analysis of EF depleted Ewing cells have often tried to identify novel Ewing cell vulnerabilities. Among the gene targets previously identified, DKK1 and NR0B1 are two genes who are well studied and whose expression is sensitive of EF levels (26, 27). Since NR0B1 expression levels decrease and DKK1 expression levels increase following EF depletion, these genes are useful marker of total EF levels in Ewing sarcoma cells. In the time course RNA seq of A673 SMASh cells, I saw transcriptional level changes of these genes are very sensitive to changes in EF protein level. These changes are present across all cell lines I sequenced, suggesting that the gene changes observed in RNA seq were a result of

EF depletion. The core set of transcripts identified to be commonly altered across A673, SK.N.MC, and TC32 cells serves as a basis for future investigation and potential screening. Rather than focusing on a single target pooled screening of the common gene signatures may illuminate key pathways that are regulated by EF that can be leveraged as future therapeutics.

My in-vivo experiments have demonstrated a potent growth inhibition following depletion of EF with IAA treatment. The decrease in tumor volume demonstrates a clear need for the expression of EF in tumor maintenance. However, depletion of EF in cell lines never resulted in cell death only cell cycle arrest. The mechanisms causing tumor regression may be driven by processes not encountered during cell growth in media. As a result, further analysis of the changes occurring in vivo because of EF depletion is still required. TIR1 expression and subsequent EF depletion was selected against in the A673 AID^{TIR1} cohort after 4 days of IAA treatment resulting in tumor proliferation. Future in vivo work using single cell clones of $A673^{TIR1}$ or single cell clones of the A673 AID cells with more sensitive TIR1 mutants would likely prevent the selection of a subpopulations of cells with TIR1 and show improved tumor regression.

The N terminus of EF has been implicated in transcriptional activation and LC dependent phase separation (42, 42). Expressing exogenous EF constructs in the setting of endogenous EF depletion, allowed me to test the functionality of different portions of the N-terminal of EWS in Ewing sarcoma cells. While prior studies have associated distinct transcriptional signatures with the N and C terminal portion of the EWS portion of the translocation (45),

my data suggest that these regions are functionally redundant in driving proliferation. However, deletions from each end of EWS showed a preference for the first 75 aa in EWS. While no individual portion of this span was required, loss of this entire region resulted in non-functional EF constructs. A minimal rescue construct consisting of exon 1-5 showed a decreased ability to rescue proliferation when 2 tyrosines were mutated to serines and lost all proliferative drive once 3 tyrosines were mutated. These finding suggest that there may be a minimal number of tyrosines required for EF function. Additional constructs probing mutation of sets of 2 or 3 tyrosines across exons 1-5 may help identify if the tyrosines with these exons are redundant or if any individual set of tyrosine are uniquely essential for proliferation.

There is a clear need for additional investigation on the mechanisms behind EF driven proliferation in Ewing cell lines. My proliferation studies point to a redundancy between the first seven exons of EWS, however the exons do not seem to be equally necessary for proliferation. While the relative tyrosine to amino acid ratio between all individual exons is similar, there is a clear preference for retention of the first four exons. In vitro studies of the comparing the ability of different exons to mediate LC interactions may illuminate the reasons for the preference of exon 1-4. These future studies are of particular interest since alignment of FUS and EWS aligns the previously identified FUS LC core with exon 4 of EWS.

The LC of FUS has been a more heavily studied than EWS and can be involved in some Ewing sarcoma translocation. For this reason, I tested to see if FUS-ETS translocations would be able to substitute as proliferative driver for EWS-FLI1 in Ewing cell lines. Surprisingly, neither FUS-FLI1or FUS-ERG was able to drive long term proliferation in EF driven Ewing cell lines. This data suggests there may be selectivity for different LC domains of FET proteins. These results are particularly surprising given that FUS and EWS have both been identified in isoxazole precipitated granules and both can bind the CTD of RNA polymerase II (38-40). Further characterization of EWS LC interactions may reveal unique interactions and binding partners. Additionally, this data suggests that EWS and FUS driven Ewing tumors may have not be driven by the same transcriptional programs. Comparison of transcriptional signatures between FUS and EWS driven Ewing sarcoma tumors may reveal key genes that specific to one of these two FET proteins.

Here I have shown that depletion of EF in Ewing sarcoma cells leads to proliferation defect due to cells accumulating in the G1 phase of the cell cycle. EF depletion leads to both upregulation and downregulation of various genes across Ewing cell lines but appear to have a common core set of genes. Proliferation can be maintained through endogenous EF depletion through constitutive exogenous EF expression or rescued through endogenous EF expression by washout. These results show EF as a key regulator of G1/S and proliferation in Ewing cells. Additionally, EF expression is necessary for tumor maintenance and EF depletion leads to tumor regression in vivo.

Using proliferation as a readout of EF function, I tested a library of EF truncation and mutants. My data suggests that no single exon of EWS is necessary for proliferation if a sufficient portion of EF is expressed. Yet, there appears to be a lower tolerance for loss of the first 4 exons of EWS over exon 5, 6, &7. It is possible that the N terminal region of EWS is more important for orchestrating interactions that result in EF oncogenic function. Further characterization of portions of the EWS disordered region and its ability to form condensates may help illuminate the preference for the N-terminal portion.

CHAPTER FIVE
Experimental Procedures

Antibody List:

Antibody	Manufacturer	Catalogue #
anti-FLI1 (Rabbit)	Abcam	133485
anti-B actin (Mouse)	Cell Signaling	3700S
anti-FLAG M2 (Mouse)	Sigma-Aldrich	F3165
anti-Cyclin D1 (Rabbit)	Abcam	134175
HRP Linked anti-rabbit IgG (Horse)	CST	7074
HRP Linked anti-mouse IgG (Horse)	CST	7076
anti-FLI1 (Rabbit)	Abcam	133485

Oligo Lists:

qPCR Oligo	Sequence
TBP_RT_1f	gaa cat cat gga tca gaa caa ca
TBP_RT_1r	ata ggg att ccg gga gtc at

NR0B1_RT_F	Aagccatcaagtgctttctttc
NR0B1_RT_R	Cctgaatgtacttcacgcactg
DKK1_RT_F	Caggcgtgcaaatctgtct
DKK1_RT_R	Aatgattttgatcagaagacacacata

CRISPRa sgRNA oligos	**Sequence**
sgSAM_CyclinD1_F1	CACCGACTCCGCCGCAGGGCAGGCG
sgSAM_CyclinD1_R1	AAACCGCCTGCCCTGCGGCGGAGTC
sgSAM_CyclinD1_F2	CACCGCTATGAAAACCGGACTACAG
sgSAM_CyclinD1_R2	AAACCTGTAGTCCGGTTTTCATAGC
sgSAM_CyclinD1_F3	CACCGGCGCCTCAGGGATGGCTTTT
sgSAM_CyclinD1_R3	AAACAAAAGCCATCCCTGAGGCGCC

<u>Construct Oligos:</u>

Primer	**Sequence**
pLVX_EF_F2 (pLVX EF)	**TCGCTAGCGCTACCGGACTCAGAT**

	CACCACCATGGCGTCCAC
pLVX_R2	**GGGCCCGCGGTACCGTCGACTGCAGTCAGTAGTAGCTGCCTAAGtgtgaaggcacgtgg**
pLVX_EF_ΔEx2_F (pLVX_EFdel12)	**TCGCTAGCGCTACCGGACTCAGATCACCACCATGtacagtgcttacaccgcccagcc**
pLVX_R2	**GGGCCCGCGGTACCGTCGACTGCAGTCAGTAGTAGCTGCCTAAGtgtgaaggcacgtgg**
pLVX_EF_F2 (pLVX_EFdel3)	**TCGCTAGCGCTACCGGACTCAGATCACCACCATGGCGTCCAC**
pLVX_EF_ΔEx3_R	**gttgcccatatgcgccctgctgcgctgc**
pLVX_EF_ΔEx3_F	**gcgcagcagggcgcatatgggcaacaaagctatggaac**
pLVX_R2	**GGGCCCGCGGTACCGTCGACTGCAGTCAGTAGTAGCTGCCTAAGtgtgaaggcacgtgg**

pLVX_EF_F2 (pLVX_EFdel4)	**TCGCTAGCGCTACCGGACTCAGATCACCACCATGGCGTCCAC**
pLVX_EF_ΔEx4_R	**gagtagtataaccctgggtggtctgtgcatat**
pLVX_EF_ΔEx4_F	**cagaccacccagggttatactactccaactgccccc**
pLVX_R2	**GGGCCCGCGGTACCGTCGACTGCAGTCAGTAGTAGCTGCCTAAGtgtgaaggcacgtgg**
pLVX_EF_F2 (pLVX_EFdel5)	**TCGCTAGCGCTACCGGACTCAGATCACCACCATGGCGTCCAC**
pLVX_EF_ΔEx5_R	**ttccatcctgcggagtgggaggctgtccataag**
pLVX_EF_ΔEx5_F	**cagcctcccactccgcaggatggaaacaagcc**
pLVX_R2	**GGGCCCGCGGTACCGTCGACTGCAGTCAGTAGTAGCTGCCTAAGtgtgaaggcacgtgg**
pLVX_EF_F2 (pLVX_EFdel6)	**TCGCTAGCGCTACCGGACTCAGATCACCACCATGGCGTCCAC**
pLVX_EF_ΔEx6_R	**gtgtagaggaatatcttgtaggtgcagtggctgctgg**
pLVX_EF_ΔEx6_F	**gcacctacaagatattcctctacacagccgactagt**

pLVX_R2	**GGGCCCGCGGTACCGTCGACTGCAGTCAGTAGTAGCTGCCTAAGtgtgaaggcacgtgg**
pLVX_EF_F2 (pLVX_EFdel7)	**TCGCTAGCGCTACCGGACTCAGATCACCACCATGGCGTCCAC**
pLVX_EF_ΔEx7_R	**cataagaagggttgctggtaggagggtaggatgg**
pLVX_EF_ΔEx7_F	**cctcctaccagcaacccttcttatgactcagtcagaagagg**
pLVX_R2	**GGGCCCGCGGTACCGTCGACTGCAGTCAGTAGTAGCTGCCTAAGtgtgaaggcacgtgg**
pLVX_EF_ΔEx2,3_F (pLVX_EFdel13)	**TCGCTAGCGCTACCGGACTCAGATCACCACCATGgcatatgggcaacaaagctatggaac**
pLVX_R2	**GGGCCCGCGGTACCGTCGACTGCAGTCAGTAGTAGCTGCCTAAGtgtgaaggcacgtgg**
pLVX_EF_ΔEx2,4_F (pLVX_EFdel14)	**TCGCTAGCGCTACCGGACTCAGATCACCACCATGggttatactactccaactgcccc**

pLVX_R2	**GGGCCCGCGGTACCGTCGACTGCAGTCAGTAGTAGCTGCCTAAGtgtgaaggcacgtgg**
pLVX_EF_ΔEx1,5_F (pLVX_EFdel15)	**TCGCTAGCGCTACCGGACTCAGATCACCACCATGccgcaggatggaaacaagcc**
pLVX_R2	**GGGCCCGCGGTACCGTCGACTGCAGTCAGTAGTAGCTGCCTAAGtgtgaaggcacgtgg**
pLVX_EF_Ex7_F (pLVX_7only)	**CGCTAGCGCTACCGGACTCAGATACCACCATGtattcctctacacagccgactagttatg**
pLVX_R2	**GGGCCCGCGGTACCGTCGACTGCAGTCAGTAGTAGCTGCCTAAGtgtgaaggcacgtgg**
pLVX_EF_F2 (pLVX_EFdel67)	**TCGCTAGCGCTACCGGACTCAGATCACCACCATGGCGTCCAC**
pLVX_EF_ΔEx6,7_R	**cataagaagggtttcttgtaggtgcagtggctgctgg**
pLVX_EF_ΔEx6,7_F	**gcacctacaagaaacccttcttatgactcagtcagaagag**

pLVX_R2	**GGGCCCGCGGTACCGTCGACTGCAGTCAGTAGTAGCTGCCTAAGtgtgaaggcacgtgg**
pLVX_EF_F2 (pLVX_EFdel57)	**TCGCTAGCGCTACCGGACTCAGATCACCACCATGGCGTCCAC**
pLVX_EF_ΔEx5,7_R	**cataagaagggttagtgggaggctgtccataagaag**
pLVX_EF_ΔEx5,7_F	**cagcctcccactaacccttcttatgactcagtcagaagag**
pLVX_R2	**GGGCCCGCGGTACCGTCGACTGCAGTCAGTAGTAGCTGCCTAAGtgtgaaggcacgtgg**
pLVX_EF_F2 (pLVX_EFdel57)	**TCGCTAGCGCTACCGGACTCAGATCACCACCATGGCGTCCAC**
pLVX_EF_ΔEx4,7_R	**cataagaagggttctgggtggtctgtgcatatcc**
pLVX_EF_ΔEx4,7_F	**cagaccacccagaacccttcttatgactcagtcagaag**
pLVX_R2	**GGGCCCGCGGTACCGTCGACTGCAGTCAGTAGTAGCTGCCTAAGtgtgaaggcacgtgg**

pLVX_EF_F2 (pLVX_EFYS12)	**TCGCTAGCGCTACCGGACTCAGATCACCACCATGGCGTCCAC**
pLVX_YS(1-2)_R	**tgtaagcactgtagccctgctgcgc**
pLVX_YS(1-2)_F	**gcgcagcagggctacagtgcttac**
pLVX_R2	**GGGCCCGCGGTACCGTCGACTGCAGTCAGTAGTAGCTGCCTAAGtgtgaaggcacgtgg**
pLVX_EF_F2 (pLVX_EFYS3)	**TCGCTAGCGCTACCGGACTCAGATCACCACCATGGCGTCCAC**
pLVX_YS(3)_R	**tggaagcactggagccctgctgcgc**
pLVX_YS(3)_F	**gcgcagcagggctccagtgcttcc**
pLVX_R2	**GGGCCCGCGGTACCGTCGACTGCAGTCAGTAGTAGCTGCCTAAGtgtgaaggcacgtgg**
pLVX_EF_F2 (pLVX_EFYS4)	**TCGCTAGCGCTACCGGACTCAGATCACCACCATGGCGTCCAC**
pLVX_YS(4)_R	**gttgcccagatgcctgggtggtctg**
pLVX_YS(4)_F	**cagaccacccaggcatctgggcaa**

pLVX_R2	**GGGCCCGCGGTACCGTCGACTGCAGTCAGTAGTAGCTGCCTAAGtgtgaaggcacgtgg**
pLVX_EF_F2 (pLVX_EFY13)	**TCGCTAGCGCTACCGGACTCAGATCACCACCATGGCGTCCAC**
pLVX_YS(3)_4R	**gttgcccatatgcctgggtggtctg**
pLVX_YS(3)_4F	**cagaccacccaggcatatgggcaa**
pLVX_R2	**GGGCCCGCGGTACCGTCGACTGCAGTCAGTAGTAGCTGCCTAAGtgtgaaggcacgtgg**
pLVX_EF_F2 (pLVX_EFYS13del4)	**TCGCTAGCGCTACCGGACTCAGATCACCACCATGGCGTCCAC**
pLVX_YS(1-3)Δ_R	**gagtagtataaccctgggtggtctgtgcaga**
pLVX_YS(1-3)Δ_F	**cagaccacccagggttatactactccaactgccccc**
pLVX_R2	**GGGCCCGCGGTACCGTCGACTGCAGTCAGTAGTAGCTGCCTAAGtgtgaaggcacgtgg**
pLVX_EF_F2 (pLVX_EFYS14)	**TCGCTAGCGCTACCGGACTCAGAT**

	CACCACCATGGCGTCCAC
pLVX_YS(1-4)_R	**gagtagtataaccctgggtggtctgtgcaga**
pLVX_YS(1-4)_F	**cagaccacccagggttatactactccaactgccccc**
pLVX_R2	**GGGCCCGCGGTACCGTCGACTGC AGTCAGTAGTAGCTGCCTAAGtgtga aggcacgtgg**
pLVX_EF_F2 (pLVX_EFYF14)	**TCGCTAGCGCTACCGGACTCAGAT CACCACCATGGCGTCCAC**
pLVX_YF_R	**ggagtagtataaccagtgggaggctgtccaaaaga**
pLVX_YF_F	**agcctcccactggttatactactccaactgc**
pLVX_R2	**GGGCCCGCGGTACCGTCGACTGC AGTCAGTAGTAGCTGCCTAAGtgtga aggcacgtgg**
pLVX_EF_F2 (pLVX_EFYS12del67)	**TCGCTAGCGCTACCGGACTCAGAT CACCACCATGGCGTCCAC**
pLVX_EF_ΔEx6,7_R	**cataagaagggtttcttgtaggtgcagtggctgctgg**
pLVX_EF_ΔEx6,7_F	**gcacctacaagaaacccttcttatgactcagtcagaag ag**

pLVX_R2	**GGGCCCGCGGTACCGTCGACTGCAGTCAGTAGTAGCTGCCTAAGtgtgaaggcacgtgg**
pLVX_EF_F2 (pLVX_EFYS3del67)	**TCGCTAGCGCTACCGGACTCAGATCACCACCATGGCGTCCAC**
pLVX_EF_ΔEx6,7_R	**cataagaagggtttcttgtaggtgcagtggctgctgg**
pLVX_EF_ΔEx6,7_F	**gcacctacaagaaacccttcttatgactcagtcagaagag**
pLVX_R2	**GGGCCCGCGGTACCGTCGACTGCAGTCAGTAGTAGCTGCCTAAGtgtgaaggcacgtgg**
pLVX_EF_F2 (pLVX_EFYS13del67)	**TCGCTAGCGCTACCGGACTCAGATCACCACCATGGCGTCCAC**
pLVX_EF_ΔEx6,7_R	**cataagaagggtttcttgtaggtgcagtggctgctgg**
pLVX_EF_ΔEx6,7_F	**gcacctacaagaaacccttcttatgactcagtcagaagag**
pLVX_R2	**GGGCCCGCGGTACCGTCGACTGCAGTCAGTAGTAGCTGCCTAAGtgtga**

	aggcacgtgg
pLVX_EF_F2 (pLVX_EWSERG)	**TCGCTAGCGCTACCGGACTCAGATCACCACCATGGCGTCCAC**
pLVX_EE_ERG_ER	**GCTCATATGGTAActgctgcccgtagctg**
pLVX_ERG_F	**tacgggcagcagTTACCATATGAGCCCCCCAGGAGA**
pLVX_ERG_R	**GGGCCCGCGGTACCGTCGACTGCAGTTAGTAGTAAGTGCCCAGATGAGAAGGCA**
pLVX_FF_F (pLVX_FUSFLI1)	**TCGCTAGCGCTACCGGACTCAGATCACCACCatggcctcaaacg**
pLVX_R2	**GGGCCCGCGGTACCGTCGACTGCAGTCAGTAGTAGCTGCCTAAGtgtgaaggcacgtgg**
pLVX_FF_F (pLVX_FUSERG)	**TCGCTAGCGCTACCGGACTCAGATCACCACCatggcctcaaacg**
pLVX_FUS_ERG_R	**GCTCATATGGTAAaccaaatttattgaagccaccacg**

pLVX_FUS_ERG_F	**aataaatttggtTTACCATATGAGCCCCC CAGGA**
pLVX_ERG_R	**GGGCCCGCGGTACCGTCGACTGC AGTTAGTAGTAAGTGCCCAGATGA GAAGGCA**
Common_EF_F (pZIP_EFSMASh)	**gtaaagaattaattcccgtatacaACCACCATG GCGTCC**
FLI1_SM_GSG_R	**GGGTAAGTGCTGTCCAGATCCGTA GTAGCTGCCTAAGtgtgaaggc**
Cutless_SM_F	**AGGCAGCTACTACGGATCTGGAC AGCACTTACCCGGCG**
Cutless_SM_Stp_R	**tcttacccgtcattggctgtccagaTCAGTGCGT CAGGGTGACTGC**

Cell Culture:

A673 (CRL-1598), SK-N-MC (HTB-10) were purchased from ATCC and TC32 (Children's Oncology Group) were cultured in RPMI 1640 media (Sigma-Aldrich R7256) with 10% FBS (#35-150-CV, Corning), 1% Pen-Strep (Sigma P4332), 1% L-glutamine (Sigma-Aldrich

G7513). HEK 293-F cells (Thermo R79007) were cultured in DMEM (Sigma-Aldrich D6429) with 10% FBS, 1% Pen-Strep (Sigma P4332), and 1% L-glutamine (Sigma-Aldrich G7513). All cell lines were maintained in an incubator at 37°C with 5% CO2. Cell lines were periodically tested for mycoplasma and had their identities verified by STR profiling.

Cell Cycle Analysis:

Cell cycle status was determined using Guava Cell Cycle reagent (Luminex 4500-0220) according to the manufacturer's instructions. Briefly, cells were washed with PBS, fixed using 70% ethanol, and incubated with cell cycle reagent for 30 min at room temperature. Flow cytometry analysis was performed using Guava easyCyte HT Flow Cytometer and analyzed with Guava InCyte software (Millipore).

Cell Titer Glow:

TC32 cells were plated at $7.5x10^3$ cells per well in triplicate for each treatment condition in 96 well white bottom plates (Fischer Scientific 3610). Cells were maintained on compound for 5 days. ATP was measured using CellTiter-Glo Luminescent Viability Assay (Promega G7573) per the manufacturer's instruction. Plates were analyzed on a Cytation Plate reader (BioTek).

CRISPRa Cell Line Generation:

Control or CCND1 guide sequences were obtained from the Human CRISPR Activation Library (49) and synthesized by Integrated Data Technologies. Guides were cloned in the LentiSAMv2 Backbone (Addgene #75112) as described previously (49). TC32 SMASh cells

were transduced at an MOI of 0.7 with MS2-P65-HSF1 plasmid (Addgene # #89308) and selected with Hygromicin B (Thermo Fisher 10687010). Selected TC32-MPH cells were transduced with LentiSAMv2 containing CCND1 or control sgRNA at an MOI of 0.3 and selected using Blasticidin (Thermo Fisher NC9016621).

EWS-FLI1 Degron Cell Line Generation:

Ewing cell lines were transfected with LentiCRISPR_v2 (Addgene #52961) and corresponding sgRNA& donor plasmid for targeting of degron tags. Individual clones were picked after neomycin selection and proper targeting of a single allele with no duplication was verified by sanger sequencing. Sequenced clones were verified for depletion by western blot. AID cell lines were transduced with pLVX_V5-TIR1_ZsGreen.

Generation of EWS-FLI1 expression plasmids & Lentivirus Production:

EWS-FLI1 constructs were expressed using a CMV driven pLVX-IRES-puro (Clontech) backbone. EWS-FLI1 gene blocks (IDT) used as template for expression constructs. Plasmid inserts were amplified using Cloneamp HiFi PCR Mix (ClonTech 6329298) or Kapa HiFi HS Mix (KapaBiosystems KK2602). Plasmids were assembled with NEB Assembly Mastermix (NEB E2621X). Plasmids were transformed into Stbl3 E.coli, isolated as single colonies, and sequence verified. Lentivirial plasmids were generated by transfecting 293-F cells with EWS-FLI1 plasmid, psPAX2 (Addgene plasmid #12260), and pMD2.G (Addgene plasmid #12259) in a ratio (4:3:1) using TransIT®-LT1Transfection reagent (MIR 2304, Mirus Bio) as described by the manufacturer.

EWS-FLI1 Construct Cell Doubling Assay:

TC32 or SK-N-MC cells were transduced with EWS-FLI1 construct lentivirus and selected with puromycin (Sigma P8833). Cell lines with validated expression of EWS-FLI1 construct were plated with $1x10^6$ cells in duplicate 6cm plates for each treatment condition. Cells were serially passed and counted every 3 days using the ViCell XR cell counter (Beckman Coulter). Alternatively, cells were counted in a 1:20 dilution with Luminex ViaCount reagent (Luminex 4000-0040) using the Guava easyCyte HT Flow Cytometer according to the manufacturer's instructions (Millipore).

RNA Extraction & qPCR:

RNA was isolated using Trizol reagent (Thermo Fisher 15596018) and the Directzol RNA Midi Prep Plus Kit (Zymo R2071) according to the manufacturer's instructions. RNA sample QC, library prep, and sequencing were done by the UTSW Next Generation Sequence Core or by BGI.

cDNA was prepared using Applied Biosystems High Capacity cDNA Reverse Transcription Kit (Fischer Scientific #43-688-14). qPCR primers are listed in the primer and antibody sheet. qPCR reactions used SYBR Green PCR Master mix (Thermo Fischer 4309155) and read on QuantStudio 3 RealTime PCR System (Thermo Fischer).

Western Blot Analysis:

Western blotting was performed using standard methods. Immobilon-P PVDF membranes (Milipore*)* were used for protein transference and then blocked using 5% Milk in PBS for 1h

at RT. Primary antibodies were incubated for 1h at RT diluted 1:1000 in 5% BSA in PBS-Tween (0.1%). Antibodies used were anti-FLI1 rabbit [ERP4646] mAb (Abcam # 133485), and anti-β-actin (8H10D10) mouse mAb (#3700, Cell Signaling Technologies). Membrane was washed with PBS-Tween (0.1%) three times for 5 minutes each wash. Secondary antibodies were incubated for 40 min at RT using HRP Linked Horse anti-rabbit IgG (H+L) (CST #7074), and HRP linked anti-mouse IgG (H+L) (CST #7076), at a dilution of 1:2500.

Evaluation of Xenograft Growth & Tumor Sample Processing:

Mouse experiments were performed in accordance with IACUC guidelines at the animal facility in UTSW. Xenografts were generated as previously described (48). Nude or NSG mice were injected with 1 million cells @ 1:1 mix with Geltrex Membrane Matrix (Thermo Fisher A1413202). Xenografts were measured every 3 days until palpable tumors were identified. Mice were treated every twelve hours with an auxin solution: 10% DMSO, 10% Kolliphor EL (Sigma-Aldrich C5135), 80% 0.1M Na carbonate buffer (pH 9.5). Mice were sacrificed 2h after their final dose of either vehicle or IAA. Extracted tumors were divided into pieces for snap freezing in liquid nitrogen or formalin fixation. Frozen tumor pieces were ground into a fine powder using a mortar and pestle and resuspended in RIPA buffer and homogenized. Plasma was isolated by collecting whole blood in Microtainer K2 EDTA tubes (BD 365972) and centrifuging for 15 min at 2000x g in a 4°C centrifuge.

BIBLIOGRAPHY

1. Ewing, J. *Diffuse endothelioma of bone*. Proc NY Pathol Soc 1921. **21**: p.17–24

2. Ries L.A.G., et al. *Cancer Incidence and Survival among Children and Adolescents: United States SEER Program 1975-1995*, National Cancer Institute, SEER Program. NIH Pub. No. 99-4649. Bethesda, MD, 1999.

3. Grier, H. E., et al. *Addition of Ifosfamide and Etoposide to Standard Chemotherapy for Ewing's Sarcoma and Primitive Neuroectodermal Tumor of Bone*. N Engl J Med, 2003. **348**(8): p.694-701

4. Gaspar, N. et al., *Ewing Sarcoma: Current Management and Future Approaches Through Collaboration***.** Journal of Clinical Oncology 2015. **33**(27): p.3036-3046

5. Marina, N. M., et al., *Longitudinal Follow-up of Adult Survivors of Ewing Sarcoma: A Report from the Childhood Cancer Survivor Study.* Cancer. 2017. **123**(13): p.2551-60.

6. Delattre, O., et al., *Gene fusion with an ETS DNA-binding domain caused by chromosome translocation in human tumours.* Nature, 1992. **359**(6391): p. 162-5.

7. Delattre, O., et al. *The Ewing Family of Tumors -- A Subgroup of Small-Round-Cell Tumors Defined by Specific Chimeric Transcripts.* NEJM, 1994. **331**: p. 294-299

8. Shing, D.C., et al., *FUS/ERG gene fusions in Ewing's tumors*. Cancer Res, 2003. **63**(15): p.4568-76

9. Anderson, J.L., et al., *Pediatric Sarcomas: Translating Molecular Pathogenesis of Disease to Novel Therapeutic Possibilities.* Pediatr Res, 2015. **72**(2): 112-121

10. Brohl, A.S., et al., *The genomic landscape of the Ewing Sarcoma family of tumors reveals recurrent STAG2 mutation.* PLoS Genet, 2014. **10**(7): p. e1004475.

11. Crompton, B.D., et al., *The genomic landscape of pediatric Ewing sarcoma.* Cancer Discov, 2014. **4**(11): p. 1326-41.

12. Tirode, F., et al., *Genomic landscape of Ewing sarcoma defines an aggressive subtype with co-association of STAG2 and TP53 mutations.* Cancer Discov, 2014. **4**(11): p. 1342-53.

13. May, W.A., et al., *Ewing sarcoma 11;22 translocation produces a chimeric transcription factor that requires the DNA-binding domain encoded by FLI1 for transformation.* Proc Natl Acad Sci U S A, 1993. **90**(12): p. 5752-6.

14. May, W.A., et al., *The Ewing's sarcoma EWS/FLI-1 fusion gene encodes a more potent transcriptional activator and is a more powerful transforming gene than FLI-1.* Mol Cell Biol, 1993. **13**(12): p. 7393-8.

15. Lessnick, S.L., et al., *Multiple domains mediate transformation by the Ewing's sarcoma EWS/FLI-1 fusion gene.* Oncogene, 1995. **10**(3): p. 423-31.

16. Lessnick S.L., et al., *The Ewing's sarcoma oncoprotein EWS/FLI induces a p53-dependent growth arrest in primary human fibroblasts.* Cancer Cell, 2002; **1**: p.393–401

17. Zwerner J.P., et al., *EWS/FLI function varies in different cellular backgrounds.* Exp Cell Res 2003, **290**: p.414–9

18. Riggi N., et al., *Development of Ewing's sarcoma from primary bone marrow-derived mesenchymal progenitor cells*. Cancer Research. 2005. **65**: p.11459–11468.

19. Riggi N., et al., *EWS-FLI-1 expression triggers a Ewing's sarcoma initiation program in primary human mesenchymal stem cells*. Cancer Research. 2008. **68**: p.2176–2185

20. Miyagawa, Y., et al., *Inducible expression of chimeric EWS/ETS proteins confers Ewing's family tumor-like phenotypes to human mesenchymal progenitor cells.* Mol Cell Biol, 2008. **28**(7): p. 2125-37.

21. Tirode F. et al., *Mesenchymal Stem Cell Features of Ewing Tumors*. Cancer Cell. 2007. **11**(5): p.421-9

22. Ouchida M. et al., *Loss of tumorigenicity of Ewing's sarcoma cells expressing antisense RNA to EWS-fusion transcripts*. Oncogene, 01 Sep 1995, **11**(6): p.1049-1054

23. Tanaka K. et al., *EWS-Fli1 Antisense Oligodeoxynucleotide Inhibits Proliferation of Human Ewing's Sarcoma and Primitive Neuroectodermal Tumor Cells.* J Clin Inv, 1997, **99**(2): p239-247

24. Hu, H.M., et al., *EWS/FLI1 suppresses retinoblastoma protein function and senescence in Ewing's sarcoma cells.* J Orthop Res, 2008. **26**(6): p. 886-93.

25. Smith, R., et al., *Expression profiling of EWS/FLI identifies NKX2.2 as a critical target gene in Ewing's sarcoma.* Cancer Cell, 2006. **9**(5): p. 405-16.

26. Kinsey, M., R. Smith, and S.L. Lessnick, *NR0B1 is required for the oncogenic phenotype mediated by EWS/FLI in Ewing's sarcoma.* Mol Cancer Res, 2006. **4**(11): p. 851-9.

27. Miyagawa, Y., et al., *EWS/ETS regulates the expression of the Dickkopf family in Ewing family tumor cells.* PLoS One, 2009. **4**(2): p. e4634.

28. Gangwal, K., et al., *Microsatellites as EWS/FLI response elements in Ewing's sarcoma.* Proc Natl Acad Sci U S A, 2008. **105**(29): p. 10149-54.

29. Guillon, N., et al., *The oncogenic EWS-FLI1 protein binds in vivo GGAA microsatellite sequences with potential transcriptional activation function.* PLoS One, 2009. **4**(3): p. e4932.

30. Grunewald, T. G., V. et al., *Chimeric Ewsr1-Fli1 Regulates the Ewing Sarcoma Susceptibility Gene Egr2 Via a Ggaa Microsatellite*. Nat Genet. 2015. **47**(9): p.1073-8.

31. Riggi, N. et al., *EWS-FLI1 utilizes divergent chromatin remodeling mechanisms to directly activate or repress enhancer elements in Ewing sarcoma*. Cancer Cell, 2014. **26**(5): p. 668-681

32. Johnson, K.M., et al., *Identification of two types of GGAA-microsatellites and their roles in EWS/FLI binding and gene regulation in Ewing sarcoma.* PLoS One, 2017. **12**(11): p. e0186275.

33. Tomazou E.M. et al., *Epigenome mapping reveals distinct modes of gene regulation and widespread enhancer reprogramming by the oncogenic fusion protein EWS-FLI1*. Cell Rep. 2015. **10**(7): p.1082–1095.

34. Boulay, G., et al., *Epigenome editing of microsatellite repeats defines tumor-specific enhancer functions and dependencies*. Genes Dev, 2018. **32**(15-16): p. 1008-1019.

35. Schwartz, J.C. et al., *Biochemical Properties and Biological Function of FET Proteins*, Annu Rev Biochem. 2015. **84**: p.355-79

36. Huntley, M. A., and G. B. Golding. Simple Sequences Are Rare in the Protein Data Bank. Proteins, 2002. **48**(1): p. 134-40

37. Spahn, L., et al., *Homotypic and Heterotypic Interactions of Ews, Fli1 and Their Oncogenic Fusion Protein*. Oncogene. 2003. **22**(4): p. 6819-29

38. Kato, M., et al., *Cell-free formation of RNA granules: Low complexity sequence domains form dynamic fibers within hydrogels.* Cell. 2012 **149**: p.753–67

39. Han, T.W., et al., *Cell-free formation of RNA granules: Bound RNAs identify features and components of cellular assemblies*. Cell. 2012. **149**: p.768–79

40. Kwon, I., et al., *Phosphorylation-regulated binding of RNA polymerase II to fibrous polymers of low-complexity domains*. Cell. 2013. **155**: p.1049–60

41. Murray, D.T. et al., *Structure of FUS Protein Fibrils and Its Relevance to Self-Assembly and Phase Separation of Low-Complexity Domains.* Cell. 2017. **171**(3): p. 615-627

42. Chong, S., et al., *Imaging dynamic and selective low-complexity domain interactions that control gene transcription*. Science. 2018. **361**(6400): p. science.aar2555

43. Ng, P.K., et al., *Multiple aromatic side chains within a disordered structure are critical for transcription and transforming activity of EWS family oncoproteins*. Proc Natl Acad Sci USA, 2007. **104**(2): p.479-84

44. Boulay, G., et al., *Cancer-Specific Retargeting of BAF Complexes by a Prion-like Domain.* Cell, 2017. **171**(1): p. 163-178 e19.

45. Theisen, E.R., et al., *Transcriptomic analysis functionally maps the intrinsically disordered domain of EWS/FLI and reveals novel transcriptional dependencies for oncogenesis.* Genes Cancer, 2019. **10**(1-2): p. 21-38.

46. Chung, H. K., et al., *Tunable and Reversible Drug Control of Protein Production Via a Self-Excising Degron*. Nat Chem Biol. 2015. **11**(9): p.13-20.

47. Nishimura, K. et al., *An auxin-based degron system for the rapid depletion of proteins in nonplant cells*. Nature Methods. 2009. **6**(12): p.917-922

48. Ambati, S.R. et al. *Pre-clinical efficacy of PU-H71, a novel HSP90 inhibitor, alone and in combination with bortezomib in Ewing sarcoma.* Molecular Oncology, 2013. **8**(2014): p.323-336

49. Joung, J. et al. *Genome-scale CRISPR-Cas9 knockout and transcriptional activation screening*. Nature Methods, 2017. **12**: p.828-863

50. Yesbolatova, A. et al. *The auxin-inducible degron 2 technology provides sharp degradation control in yeast, mammalian cells, and mice*. Nat Commun, 2020. **11**(5701):

Acknowledgements

I would like to thank Dr. David McFadden and members of the McFadden lab for their help, suggestions, and guidance. In particular, I would like to acknowledge Xin Bai and Florentina Moreno who did so much of the groundwork for this project before my joining the lab to this project. I would like to thank Dr. Noelle Williams and UTSW Animal Pharmacology for their assistance and collaboration in all mouse projects. I'm grateful for the Biological Chemistry graduate students and faculty for their thoughtful advice and suggestion during WIPS. Finally, I would like to thank my thesis committee members, Drs. James Amatruda, Steve McKnight, and Hongtao Yu for their helpful advice and perspectives on this project over the years.